JAHRBUCH DER GEOLOGISCHEN BUNDESANSTALT
Jb. Geol. B.-A. | ISSN 0016-7800 | Band 153 | Heft 1–4 | S. 191–224 | Wien, Dezember 2013

Nannobacteria-like Particles in an Upper Silurian Limestone from the Cellon Section (Carnic Alps/Austria)

HELGA PRIEWALDER*

12 Plates

Nannobacteria-like particles
Scanning Electron Microscope
Alticola Limestone
Upper Silurian
Cellon section
EDX

Österreichische Karte 1:50.000
Blatt 197 Kötschach

Contents

Zusammenfassung . . . 191
Abstract . . . 192
Introduction . . . 192
Characterisation of the studied sample . . . 192
Analytical Techniques . . . 193
  Preparation of the sample . . . 193
    Palynological preparation . . . 193
    HF treatment . . . 193
    HCl treatment . . . 194
    Preparation after FOLK & LYNCH (1997) . . . 194
    Ultrasound treatment . . . 194
  Sputtercoater . . . 194
  SEM . . . 194
  EDX . . . 194
Nannobacteria-like particles in the present study . . . 194
  Chemically untreated or only gently treated rock samples . . . 194
  Samples after application of hydrofluoric acid . . . 194
Discussion . . . 195
Conclusions . . . 197
Acknowledgements . . . 197
References . . . 198
Plates . . . 200

Nannobakterien-ähnliche Objekte in einem obersilurischen Kalk aus dem Cellon-Profil (Karnische Alpen/Österreich)

Zusammenfassung

Die Minerale (Apatit, Dolomit/Ankerit, Fe-Oxide, Kalzit, Pyrit, Quarz, Tonminerale) eines dunkelgrauen, laminierten Kalzisiltits aus dem Alticola-Kalk (oberes Silur) des Cellon-Profils (Karnische Alpen/Österreich) wurden bei starken Vergrößerungen (bis zu 50.000 x) im REM und EDX untersucht. Die meisten von ihnen zeigten einen Aufbau aus Kügelchen mit Durchmessern von 0,02 bis 0,1 µm.

Seit 1993 gab es Berichte über 20 bis 200 nm große Mineralkörner in terrestrischen Sedimentgesteinen und Mars-Meteoriten, in menschlichem und tierischem Blut sowie in Arterienablagerungen und Nierensteinen. Diese Gebilde wurden Nannobakterien genannt und als eine bisher unbekannte Gruppe von Bakterien beschrieben, die sowohl Minerale ausfällen und somit fossil werden konnten, als auch verschiedene Krankheiten verursachten. In der jüngeren Vergangenheit wurde ihre Entstehung durch anorganische Ausfällungen in Laborexperimenten nachgewiesen.

Auch in der vorliegenden Arbeit wird der Theorie einer Herkunft der Kügelchen aus anorganischen Prozessen gefolgt. Gestützt wird diese Annahme durch das Wachstum winziger Kalziumfluorid-Kristalle auf den Oberflächen von Kalkstücken, die einige Stunden mit Flusssäure behandelt worden waren: die Kristalle erwiesen sich als vollständig aus kugeligen Körnchen zusammengesetzt.

* HELGA PRIEWALDER: Geologische Bundesanstalt, Neulinggasse 38, 1030 Wien. helga.priewalder@geologie.ac.at

Abstract

The minerals (apatite, calcite, clay minerals, dolomite/ankerite, Fe-oxides, pyrite, quartz) in dark grey, laminated calcisiltite of the Alticola Limestone (upper Silurian) from the Cellon Section (Carnic Alps, Austria) have been examined with the SEM and EDX at high magnifications (up to 50,000 x). Most have a habit comprising minute spheres (0.02 to 0.1 µm diameter).

Since 1993, tiny mineral grains, with diameters of 20 to 200 nm, have been reported from terrestrial sedimentary rocks, from Martian meteorites, from human and animal blood, arterial plaques and kidney stones. These were termed nannobacteria and considered to be a new group of bacteria that were able both to precipitate minerals, and hence become fossilised, and to cause several diseases. During the last decade, however, an inorganic origin for such grains has been proved by detailed analysis, including experimental work.

This paper regards the theory of an inorganic formation for the spheres as the most plausible. This is supported by the formation of minute calcium fluoride crystals that grew on fragments of laminated calcisiltite within a few hours of their being coated with hydrofluoric acid. These minerals are composed entirely of tiny spheres.

Introduction

During investigations of chitinozoa from the Cellon section (Carnic Alps, Austria), minute spheres (ca. 20–200 nm = 0.02–0.2 µm diameter) were observed, comparable to the nannobacteria described by Folk (1993).

Chitinozoa are lower Palaeozoic microfossils with remarkably resistant vesicles made of organic material. They can, therefore, be extracted by standard palynological methods by the application of strong acids (HCl, HF, HNO_3). After this treatment, undissolved material remains in the fluid and is screened under a light microscope to separate the fossils for SEM examination.

However, when the acid-resistant residues of dark carbonates and shales were examined under the light microscope, it was seen that a web-like matter clinging to chitinozoan vesicles had attracted organic debris, making hand-picking of the chitinozoa very difficult. To resolve this problem, the origin of the web-like material had to be established; had it formed prior to dissolution of the samples or was it produced during acid treatment?

To investigate this, "web" material and fragments of the parent rock that had not been completely dissolved were examined in the SEM. At the same time, pieces of the original sample were treated with different chemical techniques to clean their surfaces. All the samples were then examined at 50,000 x in the SEM. This showed that no matter how the samples had been prepared, in all of them minute spheres were present. As a result, the nannobacteria-like particles (NLP; cf. Martel & Young, 2008) became the subject of a more detailed study.

Folk (1993) first reported such features, as a result of a high-magnification SEM study of travertine from the hot springs at Viterbo, Italy. Folk (1993) named the particles "nannobacteria" and pointed out that they were building up numerous mineral grains and did not just rest on the surfaces. Furthermore, Folk (1993) noted that they were also abundant in modern ooids, hardgrounds and cements from both the Bahamas and the Great Salt Lake (Utah), in Palaeozoic and Mesozoic limestones, as well as in a number of minerals such as dolomite, native sulphur, metallic sulphides, silica and clay minerals.

During the following decade, several studies on the occurrence of such nannobacteria in sedimentary rocks were published. They were found in modern aragonite cements of calcified brine-shrimp egg cases in the Great Salt Lake (Pedone & Folk, 1996), in clay minerals from an Oligocene sandstone from the subsurface of Texas (Folk & Lynch, 1997) and in all environments where carbonates are precipitated, such as marine sediments, caliches, creek calcites, speleothem calcite, spring deposits and pipe-scale (cf. Folk, 1999). Folk & Chafetz (2000) reported nannobacteria from carbonate deposits from the Lower Proterozoic and younger rocks. The tiny spheres were also present on sedimentary pyrite (framboids, euhedral crystals and metasomatic masses) from the Proterozoic up to today (Folk, 2005) and on palygorskite/sepiolite in a Texas caliche (Folk & Rasbury, 2007).

McKay et al. (1996) applied the method of Folk (1993) to a Martian meteorite and found structures that looked like the nannobacteria in terrestrial rocks (cf. Folk, 1997). A further report on nannobacteria from a Martian meteorite was given by Folk & Taylor (2002).

During the same period, Gabbott (1998) described the preservation of soft tissues of a conodont animal from an Ashgillian (Upper Ordovician) shale in terms of tiny spherical clay minerals, and Heinen et al. (2006) found piles of spherules in microbial mats from a hot spring in the Eastern Alps.

Kajander & Çiftçioglu (1998) reported tiny spheres from human and cow blood, from kidney stones and from pathological calcification of human tissues. The spheres were considered to be pathogenic germs. As a result, numerous studies in this field were carried out (cf. Martel & Young, 2008).

However, the hypothesis of an organic origin for the NLP was controversial, as they seemed to be too small to have been living cells (Cisar et al., 2000; Velimirov, 2001; Schieber & Arnott, 2003; Martel & Young, 2008; Young et al., 2009; Young & Martel, 2010; Duda, 2011).

Characterisation of the studied sample

The examined rock sample comes from the Cellon section in the central Carnic Alps, Carinthia, Austria (Walliser, 1964; Jaeger, 1975; Schönlaub, 1985, 1994, 1997; Priewalder, 1987, 1997, 2000; Kreutzer, 1992, 1994; Kreutzer & Schönlaub, 1997; Schönlaub et al., 1997: 92–99; Histon et al., 1999; Histon & Schönlaub, 1999; Brett et al., 2009). The succession was deposited in a deeper shelf facies and ranges from the Upper Ordovician to the Lower Devonian.

The sample is a dark gray, finely laminated calcisiltite with black calcitic and gray dolomitic layers that belongs to the upper part of the Alticola Limestone [*O. remscheidensis* conodont biozone = former *O. eosteinhornensis* conodont biozone, Pridoli (Histon & Schönlaub, 1999); *U. urna* chitinozoan biozone, Pridoli (Priewalder, 1997, 2000)]. The logs in Priewalder (1997, 2000) show its exact position in the section indicated by the number 149A (bed 37A of Walliser, 1964). The deposition of this bed occurred in an offshore pelagic environment with several deepening

events, ventilating currents and changing oxygen contents (HISTON & SCHÖNLAUB, 1999; BRETT et al., 2009).

SEM-examination, chemical analyses and a brief mineralogic description of the sample

13 small pieces of the laminated calcisiltite were examined thoroughly in the SEM, at a magnification of 50,000 x, and in the EDX at about 20,000 x. It has to be noted that no detailed sedimentological study of the sample has been carried out as this was beyond the scope of this article.

The specimens were either limestones or dolostones. In addition, the EDX-analyses revealed the presence of fluorapatite, silica, illite, framboids and euhedral crystals of pyrite and Fe-oxide-framboids in the limestones. In the dolostones, illite, goethite rods and spheres and Fe-oxide framboids occurred.

A characteristic feature of the limestone samples was the surface covering of large clusters of fluorapatite crystals (Pl. 6, Fig. 1). Also, in situ microfossils, such as chitinozoa and Muellerisphaerida, which are spinous spherical microfossils of uncertain systematic position, occurred. This points to abundant decaying organic material at the time of burial, suggesting the presence of bacteria involved in the break-down of organic material to produce the special biochemical microenvironments that facilitate the precipitation of apatite (LIEBIG, 1998). Another example of biomineralisation was the occurrence of numerous framboids (diameter 4–12 µm), although only a minority consisted of pyrite; the others were made up of Fe-oxides. Often these were embedded in accumulations of apatite crystals and accompanied by minute euhedral pyrite grains (Pl. 6, Fig. 4; Pl. 8, Fig. 3). Silica was a further common mineral in the apatite clusters, occurring as irregular amorphous masses (Pl. 8, Fig. 4) or thin layers. Clay minerals were also present.

The dolostone samples were composed of densely arranged euhedral dolomite and ankerite crystals with intervening layers of illite (Pl. 1, Fig. 1). A special and frequent feature were minute rod-like goethite grains with rounded tips like in WELTON (1984) that occurred as either single grains or were joined together to form aggregates of various thickness and length. Frequently, they were radially arranged, with their axes forming angles of 60°. These rods always occurred in combination with minute beads that were either loosely scattered or grouped in areas of variable sizes (Pl. 2, Figs. 1–4; Pl. 4, Figs. 1, 2). Because of their small size, it was not possible to determine the chemical composition of a single sphere with the EDX. A further peculiar phenomenon was Fe-oxide framboids that were partly or completely enveloped by illite grains, the crystallites often being just adumbrated (Pl. 5, Fig. 1).

Dolomite/ankerite crystals and goethite-rods were usually absent in the limestone samples, while fluorapatite, pyrite and amorphous silica never occurred in the dolomitic layers. One piece, however, seemed to be transitional between the two layers, uniting typical minerals of both (Pl. 3, Fig. 3).

For the whole-rock geochemistry, the following elements were determined by multiple EDX-analyses: C, O, F, Mg, Al, Si, P, S, Cl, K, Ca, Ti, Mn and Fe. Most elements were present in both the limestone and the dolostone samples, but in variable amounts. In contrast, F, P and S occurred only in the limestone, while Ti and Mn were exclusively found in the dolostone.

X-ray diffraction identified calcite, quartz, fluorapatite, ankerite, dolomite, goethite, pyrite and illite/muscovite.

Analytical Techniques

Preparation of the sample

The rock sample was crushed and then rinsed with water through sieves (mesh sizes 5 mm und 1 mm). The larger pieces were collected and then subjected to different preparation methods (see below) to investigate their impact on the rock-forming minerals. All the methods revealed conspicuous nannobacteria-like particles. Then the samples were coated with gold and examined in the SEM and EDX.

FOLK & LYNCH (1997: Figs. 7B, 7C) showed that a long duration of gold coating can lead to the creation of artefacts similar in shape and size to the nannobacteria-like particles. To prevent this, FOLK & RASBURY (2007) covered some samples with carbon, which does not generate spheres. Nevertheless, the spheres were present on the minerals (palygorskite/sepiolite) thus proving the existence of nanospheres (FOLK & RASBURY, 2007: Figs. 4, 5).

Most of the samples illustrated here were sputtered with gold for only 30 seconds in a stable position to the gold target (cf. FOLK & LYNCH, 1997).

The other samples were coated using a rotary-planetary-tilt stage. Since the two methods are completely different, their sputter times are not comparable (no thickness measurement gauge was available). Therefore, the sputter periods in the rotary-planetary-tilt stage are not specified in the description of the preparation methods below; only the terms “moderate thickness” and “excess gold” are used, where the latter indicates a sputter time twice as long as the former. Measurements of the nannobacteria-like particles suggest that a gold cover of “moderate thickness” is only slightly thicker than that used by FOLK & LYNCH (1997). For the longer time, the increase in nannobacteria-like particle size was obvious, but only already existing structures were accentuated; no new structures formed (Pl. 12, Figs. 3, 4). Moreover, sputter tests on glass slides showed that no globular gold artefacts were generated.

Palynological preparation

The samples were treated with a range of acids: initially HCl was applied to remove carbonates, then HF to eliminate silicates, then HCl again to remove hydrofluorides formed by the reaction of HF with incompletely dissolved carbonates, and finally HNO_3 to remove amorphous organic material and pyrite.

The undissolved residue provided abundant chitinozoans and other microfossils, as well as rock fragments.

REM-photos

Pl. 10, Figs. 3, 4 (gold cover: moderate thickness).
Pl. 11, Figs. 2–4; Pl. 12, Fig. 1 (gold cover: excess gold).

HF treatment

Pieces of rock were put into 51–54 % HF for 4 hours and then washed in distilled water.

REM-photos

Pl. 12, Figs. 2, 3 (gold cover: moderate thickness).
Pl. 12, Fig. 4 (gold cover: excess gold).

HCl treatment

Pieces of rock were put into 16 % HCl for 1.5–3 minutes and then washed in distilled water.

REM-photos
Pl. 1, Figs. 3, 4; Pl. 3, Figs. 3, 4; Pl. 4, Figs. 1, 2; Pl. 5, Figs. 3, 4; Pl. 11, Fig. 1 (gold cover: excess gold).

Preparation after Folk & Lynch (1997)

Pieces of rock were put into 1 % HCl for 1 minute and then washed in distilled water.

REM-photos
Pl. 1, Figs. 1, 2; Pl. 2, Figs. 1–3; Pl. 4, Figs. 3, 4; Pl. 6, Figs. 1–4; Pl. 7, Figs. 1–4; Pl. 8, Figs. 1–4; Pl. 9, Figs. 1–4; Pl. 10, Figs. 1, 2 (gold cover: thin = 30 sec. sputter time).

Ultrasound treatment

Pieces of rock were put into distilled water and then treated with ultrasound for 5 minutes.

REM-photos

Pl. 2, Fig. 4; Pl. 3, Figs. 1, 2; Pl. 5, Figs. 1, 2 (gold cover: moderate thickness).

Sputtercoater

Typ: ***Cressington 108auto***.
Sputter material: gold.
Sputter current: 40 mA.
Sputter time: 30 sec.

SEM

Typ: ***Tescan – Vega 2 XL.***

WD: 7–10 mm.

HV: 20 kV.

EDX

Typ: ***Oxford Instruments – INCA 4.15.***

WD: 30 mm.

HV: 12 kV.

Nannobacteria-like particles in the present study

In the present study, NLP were found in chemically untreated or only gently treated samples, in samples after treatment with 51–54 % HF, in undissolved samples and in the sticky, web-like matter clinging to chitinozoan vesicles after palynological preparation. In all cases, the NLP showed similar shapes and sizes; they were spherical to ovoid and their sizes ranged from about 20 to about 100 nm (0.02–0.1 µm).

Chemically untreated or only gently treated rock samples

In these samples, the NLP occurred on calcite, dolomite/ankerite, fluorapatite, illite, Fe-oxide minerals, on pyrite and on the thin coating of a chitinozoan vesicle in situ.

On dolomite/ankerite crystals (Pl. 1, Fig. 2) and on the calcite grains (Pl. 6, Fig. 2), the NLP were arranged in dense rows and layers. The illustrations in Folk (1999: Figs. 9, 16, 19), Kirkland et al. (1999: Figs. 7, 8) and Folk & Chafetz (2000: Fig. 2B) are similar.

On fluorapatite, they occurred on euhedral crystals (Pl. 9, Figs. 3, 4), as well as on anhedral crystallites forming the recrystallised shells of Muellerisphaerida (Pl. 9, Fig. 1). Their distribution here was dense and random. Occasionally, they formed chains (Pl. 9, Fig. 4) similar to those made up of pyrite and figured by Folk (2005: Fig. 9).

The illites grains wrapping the dolomite/ankerite crystals also showed randomly scattered NLP (Pl. 1, Figs. 3, 4). The mineral margins were often delicately curved by the adjoining beads.

Rodlike goethite grains always occurred in combination with NLP; these were either loosely scattered or grouped in areas of variable sizes (Pl. 2, Figs. 1–4; Pl. 3, Figs. 2, 4; Pl. 4, Figs. 1, 2). The surfaces of the rods seemed to be smooth; it was not possible to determine if they were made up of NLP as described in palygorskite/sepiolite fibres by Folk & Rasbury (2007). Some showed a slightly bulbous extension at the tips (Pl. 2, Fig. 1).

In a few cases, the nannobacteria-like particles formed mats with a thickness of one bead. They were either loosely connected to each other, leaving some space in between and occasionally forming six-rayed structures of short rods (Pl. 3, Fig. 4) or they coalesced, forming a dense thin layer (Pl. 3, Fig. 2). These images suggest that the rods originated from the NLP, but it is not clearly visible. Although no EDX-analyses were carried out at these sites, the shapes and sizes were identical with the rods and beads in many other areas of the sample, strongly suggesting that they have the same chemical composition.

Fe-oxide framboids were very common in the studied sample, especially in the limestone layers. Most of their crystallites exhibited smooth faces, but in every framboid there were several that obviously had not been completed and thus showed their original construction of densely packed spheres (Pl. 6, Fig. 3; Pl. 8, Fig. 2). Images of pyrite in Folk (2005: Figs. 4, 7, 8) are similar. Moreover, a few framboids were found with surfaces built up almost completely of NLP and short rods, very probably goethite, locally formed on them (Pl. 5, Fig. 3; Pl. 7, Figs. 1, 2). EDX-analyses showed that areas with and without rods had the same chemical composition. On the faces of some crystallites the coalescence of the beads was clearly visible (Pl. 5, Fig. 3; Pl. 7, Fig. 4).

In the Fe-oxide framboids with illite covers, both the clay minerals and the crystallites consisted of closely arranged NLP (Pl. 5, Figs. 1, 2).

Samples after application of hydrofluoric acid

The samples that were undissolved after palynological treatment were covered by a thick layer of nannobacteria-like particles when examined in the SEM. EDX-analyses revealed that these have a calcium-fluoride composition due to the reaction of hydrofluoric acid with the carbonates that had not been completely dissolved before the application of HF. The beads were closely packed and seemed to coalesce, locally forming dense and smooth areas. Some fused to larger spheres or generated rosary like chains (Pl. 11, Fig. 2).

Many illustrations of accumulations of minute spheres resemble externally these calcium fluoride beads: rusted iron (Folk, 1997: Fig. 4); lithified muscle tissue of an Ordovician conodont animal (Gabbott, 1998: Figs. 4B, 4C); calcified artery tissue, bacterial fragments and calcite precipitations (Kirkland et al., 1999: Figs. 1, 3, 4); surfaces

of pyroxene from a Martian meteorite (FOLK & TAYLOR, 2002: Figs. 6, 7, 9, 14); decaying organic tissue (SCHIEBER & ARNOTT, 2003: Figs. 1–3); surface of an ooid shell (FOLK, 2005: Fig. 12) and NLP of hydroxyapatite and calcium carbonate (MARTEL & YOUNG, 2008: Figs. 1, 2).

The tiny beads on a broken piece of undissolved rock consisting almost entirely of NLP (Pl. 12, Fig. 1) combined into larger spheres (Ø ~370–450 nm) whilst drying at about 70° C; the spheres initially had granulate surfaces but became smooth with progressive fusion. These smooth, larger spheres joined to form pairs, thus imitating the division of living cells (Pl. 11, Fig. 3). They also coalesced to form flat bodies comprising several to many discs with smooth surfaces and bumpy margins (Pl. 11, Fig. 4). The shapes of these structures were similar to the calcite particles in MARTEL & YOUNG (2008: Figs. 2c, 2d, 2f). These examples show that, under certain conditions, inorganic material may also form organic-looking features.

As a consequence of the detection of the calcium fluoride NLP, several fresh pieces of the calcisiltite sample were put into 51–54 % HF for 4 hours. After this time, the surfaces were entirely covered by minute (1–7 µm length) euhedral but – due to limited duration of precipitation – uncompleted crystals of calcium fluoride. These were completely made up of NLP with diameters of about 30 nm. The beads formed layers and several layers constituted the crystals (Pl. 12, Figs. 2–4). In some areas, the NLP were fused together, forming smooth and dense layers, but usually the spheres were clearly visible. Often, they coalesced into larger spheres and sometimes into small rings. Even if the crystal growth in hydrofluoric acid represents uncommon evidence, it clearly demonstrates the possibility of an abiotic generation of tiny spheres.

On the surfaces of a chitinozoan vesicle in-situ within limestone, a thin coating of inorganic matter formed made up by a patchy distribution of nannobacteria-like particles (Pl. 10, Figs. 1, 2). The chemical composition of these was different from the surrounding calcite and apatite, but slightly similar to both clay and Fe-oxide minerals. EDX-analyses of a web-like appendage consisting of tiny beads clinging to chitinozoan vesicles after palynological preparation (Pl. 10, Figs. 3, 4) revealed a chemical relationship to the coating of the chitinoza in situ. Moreover, sheets of minute spheres close to large agglomerations of apatite crystals on the surface of a limestone sample (Pl. 11, Fig. 1) were chemically and morphologically very similar thus indicating a provenance from the rocks for the web-like appendages. A common character of these spherules was a distinct Fe-peak in the EDX-spectra.

Discussion

Since the initial report of nannobacteria from carbonate rocks from various localities (FOLK, 1993), their nature has been strongly debated. FOLK (1993) documented not only normal calcified bacteria of about 1–3 µm length, but also tiny spheres with diameters of 0.05–0.2 µm. The latter were inferred to be bacterial spores, which are the resting states of normal bacteria in stressful environments (due to, for example, changes in chemistry, temperature, lack of nutrients, etc). Since such beads had also been found in sediments that had been deposited under normal marine conditions, FOLK (1993) speculated that they could possibly have been an independent and then living group of bacteria as well. Criteria for the assignment to the bacteria were, the form of their bodies that "*range from tiny spheres (cocci) to stubby ellipses to sausage shapes (bacilli), to chains of spheres or rods, and on to long filaments*" (FOLK, 1993: 997), the fact that the size distributions of full-sized and stressed bacteria were comparable to living bacteria and, finally, the observation that they often occurred in accumulations, as is usual for bacteria in places with a sufficient food supply. An argument against an inorganic origin was the rounded form of their bodies. Moreover, FOLK (1993) reported that the nannobacteria were enclosed in crystals of various carbonate minerals and surmised that they could have initiated carbonate precipitation.

Subsequently, PEDONE & FOLK (1996) revoked the assumption that nannobacteria were bacteria resting phases and stressed their active role in the formation of aragonite cement.

GABBOTT (1998) described the preservation of the soft tissues of a conodont animal as clay minerals from an Ashgillian (Upper Ordovician) shale. Some parts of the muscle-fibres were smooth while others showed a microgranular surface. These minute spheres (Ø 0.09–0.12 µm) were interpreted as bacterial bodies on which colloidal clay minerals had been adsorbed and hence preserved the nanobodies.

The concept of nannobacteria as formerly living but now fossilised organisms being responsible for the precipitation of various minerals was maintained in FOLK (1997, 1999, 2005), FOLK & LYNCH (1997), FOLK & CHAFETZ (2000), MILLER et al. (2004) and FOLK & RASBURY (2007). The observation that the spherules in palygorskite/sepiolite fibres are not artefacts of preparation was demonstrated by FOLK & RASBURY (2007) by using different preparation methods, such as carbon coating of the samples instead of gold, since carbon does not produce spherical artefacts.

To test the nannobacteria hypothesis, KIRKLAND et al. (1999) carried out numerous controlled calcite-precipitation experiments and added various organic substances, such as soluble organic molecules, full-size bacteria, bacteria fragments and bacteriophages, to several of their solutions. In the solutions free of organic matter, mainly euhedral calcite crystals formed, but in the remaining liquids numerous tiny beads (10–80 nm) were generated inorganically or were bacterial fragments that could not be distinguished from calcite spheres. After three days, all the tiny euhedral and rounded calcite particles had disappeared and only large (µm-scale) euhedral calcite crystals were present. When these were etched, minute spheres, like those in natural carbonates, appeared. As a result, KIRKLAND et al. (1999) concluded that the proof of biomarkers was necessary before the tiny beads could be unequivocally allocated to the bacteria. Furthermore, FOLK & RASBURY (2007) admitted that caution is required when identifying nannobacteria, since several other possibilities explaining the origin of such minute spherical objects exist.

An interesting alternative hypothesis was given by SCHIEBER & ARNOTT (2003). They performed experiments with animal and vegetable tissues that they placed in a tank with sulphate-bearing water and clay, and added naturally occurring decay bacteria, thus imitating the conditions in

subsurface sediments. The bacteria community grew very fast and led to rapid decomposition of the tissue. Initially, the organic matter was broken up by the enzymatic activity of the bacteria into pieces of tens to a few hundred nanometers. Thereafter, protein balls with diameters of 40–120 nm and very similar to the nannobacteria in shape and size were formed in large quantities. As no smaller features could be observed in the SEM, SCHIEBER & ARNOTT (2003) concluded that the next stage would be the complete dissociation of the proteins into molecules which the bacteria were then able to absorb. SCHIEBER & ARNOTT (2003) also noted that although their protein spheres had not yet been mineralised, they seemed to be stable for several weeks, time enough to become lithified as this had already been described in the fossilisation of soft tissues (GABBOTT, 1998). SCHIEBER & ARNOTT (2003) concluded that the spherules in sedimentary rocks are not fossils of small cells, but rather the mineralised transitional by-products of enzymatic bacterial decomposition of organic tissues.

On a Martian meteorite, MCKAY et al. (1996) found abundant polycyclic aromatic hydrocarbons, granular magnetite and iron sulphides and tiny carbonate spheres looking like the terrestrial nannobacteria of FOLK (1993). As these substances are all involved in biological processes, MCKAY et al. (1996) concluded that this could point to biogenic activity on ancient Mars. These conclusions caused considerable controversy within the scientific community. Microbiologists (cf. VELIMIROV, 2001) noted that such minute features were too small for viable cells. In 1998, a workshop on the definition of the minimal sizes of organisms agreed that a modern living cell requires a sphere of at least 250 ± 50 nm diameter to accommodate the basic cell machinery (KNOLL, 1999; DE DUVE & OSBORN, 1999).

HEINEN et al. (2006) studied microbial mats from a hot spring in the Eastern Alps and reported abundant tiny spheres as well as normal bacteria. Spheres with diameters of 20–60 nm formed long chains that were piled up to large clusters. Although the single beads were interpreted as being non-viable, it was envisaged that, where they are connected into chains, they represented a more complex form of organisation and thus could be able to metabolise and replicate. Unfortunately, no examination for DNA or the chemical composition of these chains has been carried out.

VELIMIROV (2001) emphasised that the term nannobacterium had never been accurately defined and also that it is not known if these features were viable cells or only fragments of larger microbes. Very small bacteria (diameters of < 200–300 nm) had been known for a long time to be a significant part of the oceanic bacterial community. They are either starvation forms in environments with an insufficient food supply, decreasing their volume by disposing of non-essential cellular material and adopting spherical shapes or they are free living bacteria (ultramicrobacteria). In natural aquatic environments, most small living bacteria with a diameter of 200 nm or less are rod-shaped, as this morphotype is better adapted to house the components necessary to keep a cell alive. Spheres of this size play a much less important role numerically (VELIMIROV, 2001).

In a paper on very small living bacteria (ultramicrobacteria), DUDA (2011) defined the smallest size of cocci at 150–200 nm (0.15–0.20 µm). These have a cell volume of < 0.1 μm^3 and a small-sized genome (3.2–0.58 Mb). Furthermore, DUDA (2011) noted that none of the NLP in rock samples hitherto had proved to be of unequivocal biogenic origin and that there had been no investigations for biomarkers in, for example, the carbonate precipitations from water-taps in FOLK (1999), which had been said to be the products of nannobacteria. DUDA (2011) also stated that it is problematic to ascribe a biogenic origin to the nannobacteria-like spheres because they cannot be cultivated which, however, is the only way to determine whether they were/are living creatures. DUDA (2011) also noted that modern cultured ultramicrobacteria belong to six phylogenetic branches of prokaryotes. They have no conjoint history of evolution and are not primordial organisms.

The medical sciences are another important field from which nannobacteria-like balls have been reported. KAJANDER & ÇIFTÇIOGLU (1998) found nannobacteria in human and cow blood and in cell culture serum. At high magnification in a SEM, the nannobacteria that KAJANDER & ÇIFTÇIOGLU (1998) cultured closely resembled in size and shape those in human kidney stones. KAJANDER & ÇIFTÇIOGLU (1998) reported that the nannobacteria precipitated apatite on their cell walls and were closely related to well know pathogenic bacteria. Thus they might cause stone formation and pathologic calcification of tissues such as arterosclerotic plaques, and might also be involved in several other diseases.

CISAR et al. (2000) examined apatite particles from blood serum, human saliva and dental plaque, but did not find traces of living organisms and interpreted the biomineralisation that formerly was attributed to nannobacteria to be an action of non-living macromolecules. Since the tiny spheres grew and proliferated in vitro, CISAR et al. (2000) assumed that the microcrystalline apatite was able to self-propagate like bacteria in cultures.

MARTEL & YOUNG (2008) repeated the experiments of KAJANDER & ÇIFTÇIOGLU (1998) and found that the calcium carbonate and calcium phosphate particles they produced in vitro, strikingly resembled the nannobacteria previously described from human and geological samples. When $CaCO_3$ precipitated from a culture medium, spherical structures had always been formed; these were preserved even after a long period of incubation. However, in cases where the culture medium was absent, the spheres gradually turned into $CaCO_3$ crystals. Thus proteins in the serum had prevented the formation of calcite crystals and forced the development of spherulitic structures. By changing the chemical conditions, the gradual appearance, size and shape of the granules could be influenced. Objects mimicking cell-divisions or cell-colonies formed and were suggestive of a biogenic origin. However, an abiotic nature was demonstrated by the fact that they survived high doses of γ-irradiation and that it was impossible to verify bacterial DNA. MARTEL & YOUNG (2008) thus concluded that such granules in meteorites and sedimentary rocks could have been the outcome of similar processes.

YOUNG & MARTEL (2010) emphasised again that nannobacteria are non-living particles made up of trivial mineral material and other matter from their environments. They just mirror the supply of chemical components. Any molecule which easily attaches to Ca-ions or apatite crystals, such as proteins, lipids or other charged particles, obstructs the process of crystallisation.

In the present study, the NLP occurred in almost all types of minerals: calcite grains (Pl. 6, Fig. 2); calcium fluorides (Pl. 11, Figs. 2–4; Pl. 12, Figs. 1–4); dolomite/ankerite crystals (Pl. 1, Fig. 2); Fe-oxide framboids (Pl. 5, Figs. 3, 4; Pl. 6., Fig. 3; Pl. 7, Figs. 1–4; Pl. 8, Figs. 1, 2); fluorapatite (Pl. 9, Figs. 1–4); goethite-rods (Pl. 2, Figs. 1–4; Pl. 3, Figs. 1–4; Pl. 4, Figs. 1, 2); mats of (goethite ?) beads (Pl. 3, Figs. 2, 4); Illite (Pl. 1, Figs. 3, 4); pyrite framboids and euhedral pyrite crystals (Pl. 8, Fig. 3); further on chitinozoa (Pl. 10, Fig. 2); web-like matter clinging to chitinozan vesicles (Pl. 10, Fig. 4); sheets of minute spheres on the surface of a limestone (Pl. 11, Fig. 1) and recrystallised Muellerisphaerida shell (Pl. 9, Fig. 1). Their sizes and shapes were quite similar: spherical to ovoid with sizes from 20 to 100 nm (0.02–0.1 µm).

In summary, there are several possible interpretations of these nano-features:

1.) They are fossil nannobacteria with a size range of 20–200 nm, as described by FOLK (1993) and KAJANDER & ÇIFTÇIOGLU (1998). However, DUDA (2011), DE DUVE & OSBORN (1999), KNOLL (1999) and VELIMIROV (2001) argued that the minimal diameter of a viable cell is at least 150–200 nm (0.15–0.20 µm). Moreover, it would be very difficult to distinguish them from artefacts, because tiny beads may be formed in many different ways (KIRKLAND et al., 1999). FOLK & RASBURY (2007: 114) admitted themselves: "*One must conclude that, at this point in the research the identification of small spheres as "nannobacteria" is definitely a judgment call*." Further, no evidence of bacterial DNA has been found. The culturable NLP in KAJANDER & ÇIFTÇIOGLU (1998), which had always been used as justification for the biological nature of the spheres, turned out to be contamination (CISAR et al., 2000; VELIMIROV, 2001; DUDA, 2011).

2.) The NLP are lithified proteins (SCHIEBER & ARNOTT, 2003). They bear a strong resemblance to the NLP in the studied sample, but here lithified proteins should be rather rare, as they usually occur in typical agglomerations at places with decaying organic material. Here, however, the spherules are predominantly bound to minerals. Only the mats of beads show a comparable aspect (Pl. 3, Fig. 2) as do the web-like appendages clinging to the chitinozoan vesicles (Pl. 10, Figs. 3, 4) and the sheets of minute spheres close to large accumulations of apatite crystals on the surface of a limestone sample (Pl. 11, Fig. 1). Some of these spheres, however, may also be lithified fragments of conventional bacteria (KIRKLAND et al., 1999).

3.) The NLP are inorganically precipitated objects. Experiments with calcium carbonate (and calcium phosphate) solutions showed that especially proteins, but also Mg^{2+}, prevented the solutions from crystallising, thus supporting the formation of spherical nannobacteria-like particles (KIRKLAND et al., 1999; CISAR et al., 2000; MARTEL & YOUNG, 2008; YOUNG & MARTEL, 2010). These nannobacteria-like particles grew and propagated like living microbes.

Such an inorganic origin of the NLP, forming the minerals seen in the studied samples seems to be the most reasonable explanation at present, though here the conditions for their formation were different. This inference is supported by the numerous tiny spheres of calcium fluoride that formed on the surfaces of samples that had not been entirely dissolved in the course of the palynological preparation (Pl. 12, Fig. 1). Even objects similar to those in MARTEL & YOUNG (2008), which mimicked cell division and cell colonies, were present (Pl. 11, Figs. 3, 4), as were chains of beads like those shown in FOLK (2005) (Pl. 11, Fig. 2). This means that, in the micro- and nannosphere, inorganically precipitated objects may have biogenic-like shapes. Another indication of an inorganic origin in the present study was tiny calcium fluoride crystals that developed within 4 hours after pieces of calcisiltite were covered by 51–54 % hydrofluoric acid. As they had not been completed due to limited duration of precipitation, it was possible to observe the process of crystal formation. These crystals were entirely made up of minute spheres which in places coalesced, thus forming smooth layers which one by one built up the crystals (Pl. 12, Figs. 2–4). It is impossible that living nannobacteria caused the precipitation of these calcium fluoride crystals, since they would not survive in hydrofluoric acid.

KIRKLAND et al. (1999) found that in solutions devoid of soluble organic material, predominantly euhedral calcite crystals with a size range of 50–800 nm formed after one day. On the other hand, masses of rounded particles (10–80 nm) were precipitated from solutions with dissolved organic matter, also after one day. Thus these experiments also demonstrated the importance of organic molecules for the precipitation of minute rounded features. However, whether the altered organic matter in the Silurian calcisiltite sample played a role in the formation of the calcium fluoride beads, or other chemical forces were acting, remains unknown.

According to KIRKLAND et al. (1999), with time, the amount of tiny calcite precipitations gradually decreased and the number and size of euhedral calcite crystals increased. After three days, all experiments, with and without organic matter, resulted in large (µm-scale) euhedral calcite crystals with smooth faces. Tiny spheres became visible again only after etching of these crystals, as is the case with natural carbonates.

Conclusions

The present study shows that nannobacteria-like particles exist. They are not artefacts of preparation, as already demonstrated by FOLK & RASBURY (2007) and were formed by inorganic precipitation processes as indicated by KIRKLAND et al. (1999), CISAR et al. (2000) and MARTEL & YOUNG (2008).

The present work has also documented that sometimes inorganic particles have shapes that are similar to living microorganisms, as stated by MARTEL & YOUNG (2008) and YOUNG & MARTEL (2010). Therefore, such features by themselves are not evidence for a biological origin.

Acknowledgements

Many thanks to Ingeborg WIMMER-FREY (Geological Survey of Austria) for carrying out the X-ray diffraction analysis of the studied sample, and for discussions and valuable comments on the mineralogy and EDX-analyses. Special thanks to Robert L. FOLK (Department of Geological Sciences, University of Texas, Austin) for his lively interest and his suggestions on the tiny spheres in my sample. To Ilka WÜNSCHE (Geological Survey of Austria) I am much obliged for the arrangement of the plates. Finally I sincerely thank Alexander Hugh RICE (Center for Earth Science, University of Vienna) for correcting my English.

References

BRETT, C.E., FERRETTI, A., HISTON, K. & SCHÖNLAUB, H.P. (2009): Silurian sequence stratigraphy of the Carnic Alps, Austria. – Palaeogeogr., Palaeoclimat., Palaeoecol., **279**, 1–28, 19 Figs., Amsterdam.

CISAR, J.O., XU, D.-Q., THOMPSON, J., SWAIM, W., HU, L. & KOPECKO, D.J. (2000): An alternative interpretation of nanobacteria-induced biomineralization. – PNAS, **97**/21, 11511–11515, 4 Figs., 1 Tab., Washington, D.C. doi: 10.1073/pnas.97.21.11511

DE DUVE, C. & OSBORN, M.J. (1999): Panel 1: Discussion. – Size Limits of Very Small Microorganisms: Proceedings of a Workshop, 5–9, Washington, D.C. (National Academy Press).

DUDA, V.I. (2011): Ultramicrobacteria. – eLS, 38 pp., 6 Figs. doi: 10.1002/9780470015902.a0000309.pub2

FOLK, R.L. (1993): SEM imaging of bacteria and nannobacteria in carbonate sediments and rocks. – J. Sediment. Petrol., **63**/5, 990–999, 23 Figs., Lawrence, KS. doi: 10.1306/D4267C67-2B26-11D7-8648000102C1865D

FOLK, R.L. (1997): Nanobacteria: surely not figments, but what under heaven are they? – naturalSCIENCE, **1**/3, 9 pp., 5 Figs., Victoria, Canada.

FOLK, R.L. (1999): Nannobacteria and the precipitation of carbonate in unusual environments. – Sedimentary Geology, **126**, 47–55, 4 Pls., Amsterdam. doi: 10.1016/S0037-0738(99)00031-7

FOLK, R.L. (2005): Nannobacteria and the formation of framboidal pyrite: Textural evidence. – J. Earth Syst. Sci, **114**/3, 369–374, 12 Figs., Bangalore. doi: 10.1007/BF02702955

FOLK, R.L. & CHAFETZ, H.S. (2000): Bacterially Induced Microscale and Nanoscale Carbonate Precipitates. – In: RIDING, R.E. & AWRAMIK, S.M. (Eds.): Microbial Sediments, 40–49, 3 Figs., 1 Tab., Berlin–Heidelberg (Springer).

FOLK, R.L. & LYNCH, F.L. (1997): The Possible Role of Nannobacteria (Dwarf Bacteria) in Clay-Mineral Diagenesis and the Importance of Careful Sample Preparation in High-Magnification SEM Study. – J. Sediment. Res., **67**/3, 583–589, 8 Figs., Tulsa.

FOLK, R.L. & RASBURY, E.T. (2007): Nanostructure of palygorskite/sepiolite in Texas caliche: possible bacterial origin. – Carbonates and Evaporites, **22**/2, 113–122, 9 Figs., Cham, Switzerland. doi: 10.1007/BF03176241

FOLK, R.L. & TAYLOR, L.A. (2002): Nannobacterial alteration of pyroxenes in martian meteorite Allan Hills 84001. – Meteoritics & Planetary Sciences, **37**/8, 1057–1069, 19 Figs., Lawrence, KS. doi: 10.1111/j.1945-5100.2002.tb00877.x

GABBOTT, S.E. (1998): Taphonomy of the Ordovician Soom Shale Lagerstätte: an Example of Soft Tissue Preservation in Clay Minerals. – Palaeontology, **41**/4, 631–667, 8 Figs., 4 Tabs., London.

HEINEN, W., GEURTS, H.P.M. & LAUWERS, A.M. (2006): Putative nanobacteria in biofilms from an alpine thermal spring. – 11 pp., 5 Figs., 1 Tab., Nijmegen. http://www.vcbio.science.ru.nl/public/pdf/fesem_nanobes-Heinen-1-variety%20in%20thermal%20springs.pdf (accessed: 16.09.2013).

HISTON, K. & SCHÖNLAUB, H.P. (1999): Taphonomy, Palaeoecology and Bathymetric Implications of the Nautiloid Fauna from the Silurian of the Cellon section (Carnic Alps, Austria). – In: FEIST, R., TALENT, J.A. & DAURER, A. (Eds.): North Gondwana: Mid-Paleozoic Terranes, Stratigraphy and Biota. – Abh. Geol. B.-A., **54**, 259–274, 18 Figs., Vienna.

HISTON, K., FERRETTI, A. & SCHÖNLAUB, H.P. (1999): Silurian Cephalopod Limestone sequence of the Cellon Section, Carnic Alps, Austria. – In: HISTON, K. (Ed.): V International Symposium Cephalopods – Present and Past. Carnic Alps Excursion Guidebook. – Ber. Geol. B.-A., **47**, 46–54, Figs. 2–5, Vienna.

JAEGER, H. (1975): Die Graptolithenführung im Silur/Devon des Cellon-Profils (Karnische Alpen). Ein Beitrag zur Gleichsetzung der Conodonten- und Graptolithenzonen des Silurs. – Carinthia II, **85**, 111–126, 5 Figs., 1 Tab., 2 Pls., Klagenfurt.

KAJANDER, E.O. & ÇIFTÇIOGLU, N. (1998): Nanobacteria: An alternative mechanism for pathogenic intra- and extracellular calcification and stone formation. – PNAS, **95**, 8274–8279, 4 Figs., 1 Tab., Washington, D.C.

KIRKLAND, B.L., LYNCH, F.L., RAHNIS, M.A., FOLK, R.L., MOLINEUX, I.J. & MCLEAN, R.J.C. (1999): Alternative origins for nannobacteria-like objects in calcite. – Geology, **27**/4, 347–350, 9 Figs., Boulder. doi: 10.1130/0091-7613(1999)027<0347:AOFNLO>2.3.CO;2

KNOLL, A. (1999): Overview. – Size Limits of Very Small Microorganisms: Proceedings of a Workshop, 1–3, Washington, D.C. (National Academy Press).

KREUTZER, L.H. (1992): Photo-Atlas of the Variscan Carbonate Sequences in the Carnic Alps (Austria/Italy). – Abh. Geol. B.-A., **47**, 129 pp., 9 Figs., 3 Tabs., 46 Pls., Vienna.

KREUTZER, L.H. (1994): Cellon Section. Facial differentiation and bathymetric environment. – In: SCHÖNLAUB, H.P. & KREUTZER, L.H. (Eds.): IUGS Subcomm. Silurian Stratigraphy, Field Meeting 1994. – Ber. Geol. B.-A., **30**, 85–88, Vienna.

KREUTZER, L.H. & SCHÖNLAUB, H.P. (1997): Cellon Section. The depositional environment. – In: SCHÖNLAUB, H.P. (Ed.): IGCP – 421 Inaugural Meeting Vienna, Guidebook. – Ber. Geol. B.-A., **40**, 99–106, Vienna.

LIEBIG, K. (1998): Fossil Microorganisms from the Eocene Messel Oil Shale of Southern Hesse, Germany. – Kaupia, **7**, 1–95, 8 Figs., 21 Pls., Darmstadt.

MARTEL, J. & YOUNG, J.D. (2008): Purported nanobacteria in human blood as calcium carbonate nanoparticles. – PNAS, **105**/14, 5549–5554, 4 Figs., Washington, D.C.

MCKAY, D.S., GIBSON JR., E.K., THOMAS-KEPRTA, K.L., VALI, H., ROMANEK, C.S., CLEMETT, S.J., CHILLIER, X.D.F., MAECHLING, C.R. & ZARE, R.N. (1996): Search for Past Life on Mars: Possible Relic Biogenic Activity in Martian Meteorite ALH84001. – Science, **273**, 924–930, Washington, D.C.

MILLER, V.M., RODGERS, G., CHARLESWORTH, J.A., KIRKLAND, B., SEVERSON, S.R., RASMUSSEN, T.E., YAGUBYAN, M., RODGERS, J.C., COCKERILL, F.R., FOLK, R.L., RZEWUSKA-LECH, E., KUMAR, V., FARELL-BARIL, G. & LIESKE, J.C. (2004): Evidence of nanobacterial-like structures in calcified human arteries and cardiac valves. – Am. J. Physiol., **287**/3, H1115–H1124, 10 Figs., 1 Tab., Bethesda, MD.

PEDONE, V.A. & FOLK, R.L. (1996): Formation of aragonite cement by nannobacteria in the Great Salt Lake, Utah. – Geology, **24**/8, 763–765, 2 Figs., 1 Tab., Boulder. doi: 10.1130/0091-7613(1996)024<0763:FOACBN>2.3.CO;2

PRIEWALDER, H. (1987): Acritarchen aus dem Silur des Cellon-Profils, Karnische Alpen, Österreich. – Abh. Geol. B.-A., **40**, 121 pp., 39 Figs., 24 Pls., Vienna.

PRIEWALDER, H. (1997): The distribution of the Chitinozoans in the Cellon Section (Hirnantian – Lower Lochkovian). – A Preliminary Report. – In: SCHÖNLAUB, H.P. (Ed.): IGCP – 421 Inaugural Meeting Vienna, Guidebook. – Ber. Geol. B.-A., **40**, 74–85, 1 Fig., Vienna.

PRIEWALDER, H. (2000): Die stratigraphische Verbreitung der Chitinozoen im Abschnitt Caradoc-Lochkovium des Cellon-Profils, Karnische Alpen (Kärnten, Österreich) – Ein vorläufiger Bericht. – Mitt. Österr. Geol. Ges., **91**, 17–29, 2 Figs., 3 Pls., Vienna.

SCHIEBER, J. & ARNOTT, H.J. (2003): Nannobacteria as a by-product of enzyme-driven tissue decay. – Geology, **31**/8, 717–720, 3 Figs., 1 Tab., Boulder. doi: 10.1130/G19663.1

SCHÖNLAUB, H.P. (1985): Das Paläozoikum der Karnischen Alpen. – In: Arbeitstagung der Geol. B.-A., **1985**, 34–52, Figs. 10–15, Vienna.

SCHÖNLAUB, H.P. (1994): Cellon Section. Lithology, Paleontology and Stratigraphy. – In: SCHÖNLAUB, H.P. & KREUTZER, L.H. (Eds.): IUGS Subcomm. Silurian Stratigraphy, Field Meeting 1994. – Ber. Geol. B.-A., **30**, 83–84, Vienna.

SCHÖNLAUB, H.P. (1997): Cellon Section. Lithology, Paleontology and Stratigraphy. – In: SCHÖNLAUB, H.P. (Ed.): IGCP – 421 Inaugural Meeting Vienna, Guidebook. – Ber. Geol. B.-A., **40**, 87–92, 1 Fig., Vienna.

SCHÖNLAUB, H.P., KREUTZER, L.H., PRIEWALDER, H., HISTON, K. & WENZEL, B. (1997): Stop 1: Cellon Section. – In: SCHÖNLAUB, H.P. (Ed.): IGCP – 421 Inaugural Meeting Vienna, Guidebook. – Ber. Geol. B.-A., **40**, 87–107, Vienna.

VELIMIROV, B. (2001): Nanobacteria, Ultramicrobacteria and Starvation Forms: A Search for the Smallest Metabolizing Bacterium. – Microbes and Environments, **16**/2, 67–77, 2 Tabs., Japan. doi:10.1264/jsme2.2001.67

WALLISER, O.H. (1964): Conodonten des Silurs. – Abh. Hess. L.-Amt Bodenforsch., **41**, 106 pp., 10 Figs., 2 Tabs., 32 Pls., Wiesbaden.

WELTON, J.E. (1984): SEM Petrology Atlas. – The AAPG methods in exploration series, **4**, 237 pp., Tulsa.

YOUNG, J.D. & MARTEL, J. (2010): Aufstieg und Fall der Nanobakterien. – Spektrum der Wissenschaft, Mikrobiologie, Oktober **2010**, 44–51, Heidelberg.

YOUNG, J.D., MARTEL, J., YOUNG, D., YOUNG, A., HUNG, C.-M., YOUNG, L., CHAO, Y.-J., YOUNG J. & WU, C.-Y. (2009): Characterization of Granulations of Calcium and Apatite in Serum as Pleomorphic Mineralo-Protein Complexes and as Precursors of Putative Nanobacteria. – PLoS ONE **4**/5: e5421, San Francisco. doi: 10.1371/journal.pone.0005421

Received: 3. September 2013, Accepted: 23. September 2013

Plate 1

Fig. 1: Overview of a dolostone sample.
The dolomite/ankerite crystals are densely arranged and surrounded by layers of illite and goethite-rods.

Fig. 2: Close-up of the surface of an ankerite crystal.
The nannobacteria-like particles are predominantly arranged in dense rows and layers.
Gold cover: thin (30 seconds sputter-time).

Fig. 3: Illitic wrapping around an dolomite/ankerite crystal.
Overview.
Box: see Pl. 1, Fig. 4.

Fig. 4: Close-up of Fig. 3 (box).
The illite consists of a pile of thin layers which are made up of tightly spaced tiny spheres. One layer seems to have the thickness of one sphere. The structures are accentuated by the gold cover.
Gold cover: excess gold.

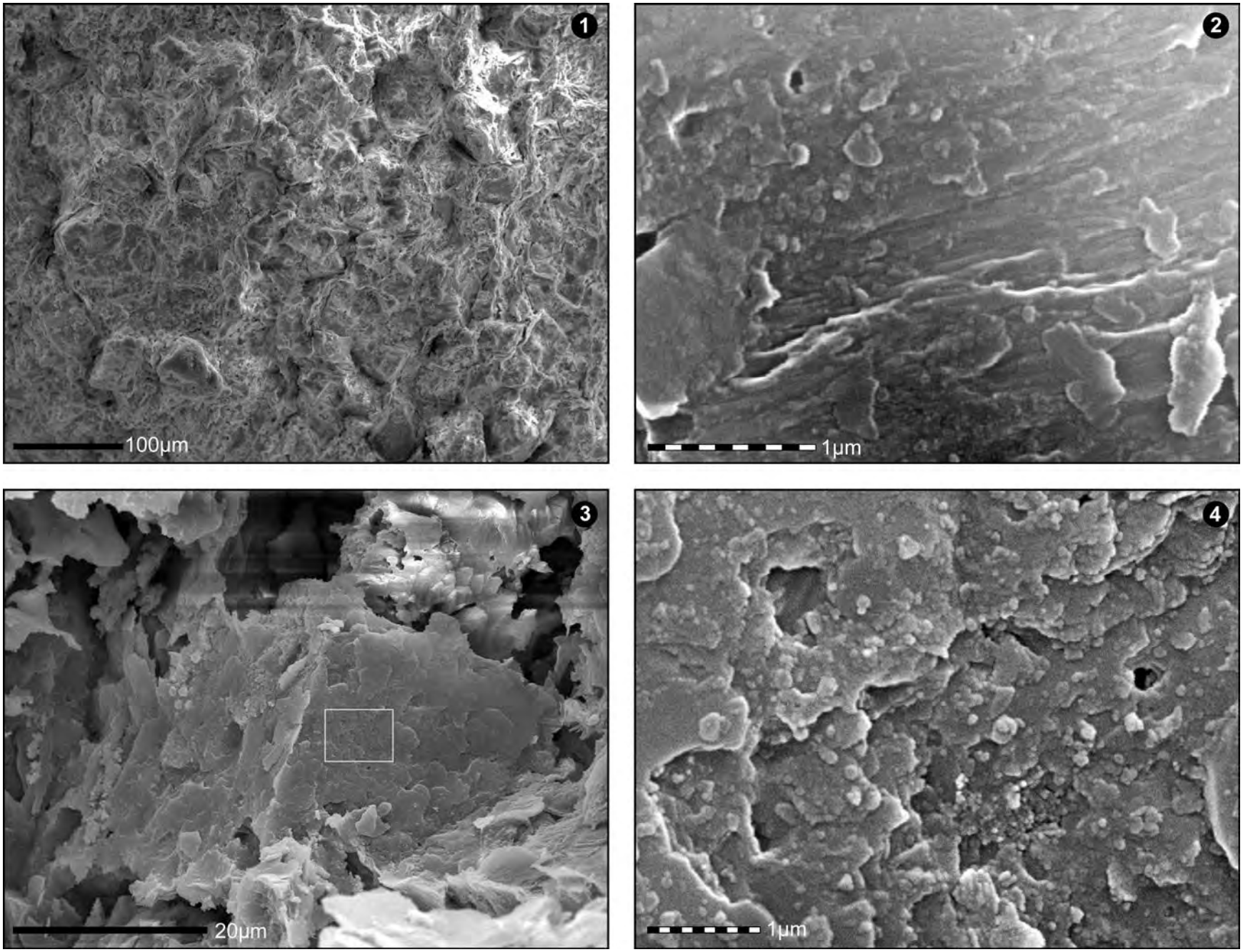
1
100µm
2
1µm
3
20µm
4
1µm

Plate 2

Fig. 1: Bunches of long thin goethite-rods.
The rods are radially arranged, their axes form angles of 60°. Some of them show a slight bulbous extension at the tips.
Gold cover: thin (30 seconds sputter-time).

Fig. 2: Accumulation of short goethite-rods.
They occur as single individuals or as bunches and are accompanied by numerous tiny beads.
Gold cover: thin (30 seconds sputter-time).

Fig. 3: Numerous nannobacteria-like particles in the center.
They are partly arranged in short rows. To the lower right, some radially grouped goethite-rods obviously merge into thin sheets.
Gold cover: thin (30 seconds sputter-time).

Fig. 4: Accumulation of goethite-rods and tiny beads.
The rods mostly occur as single individuals with rounded tips, a radial arrangement is adumbrated. The beads often coalesce to slightly larger units which may fuse to compact areas like in the lower left.
Gold cover: moderate thickness.

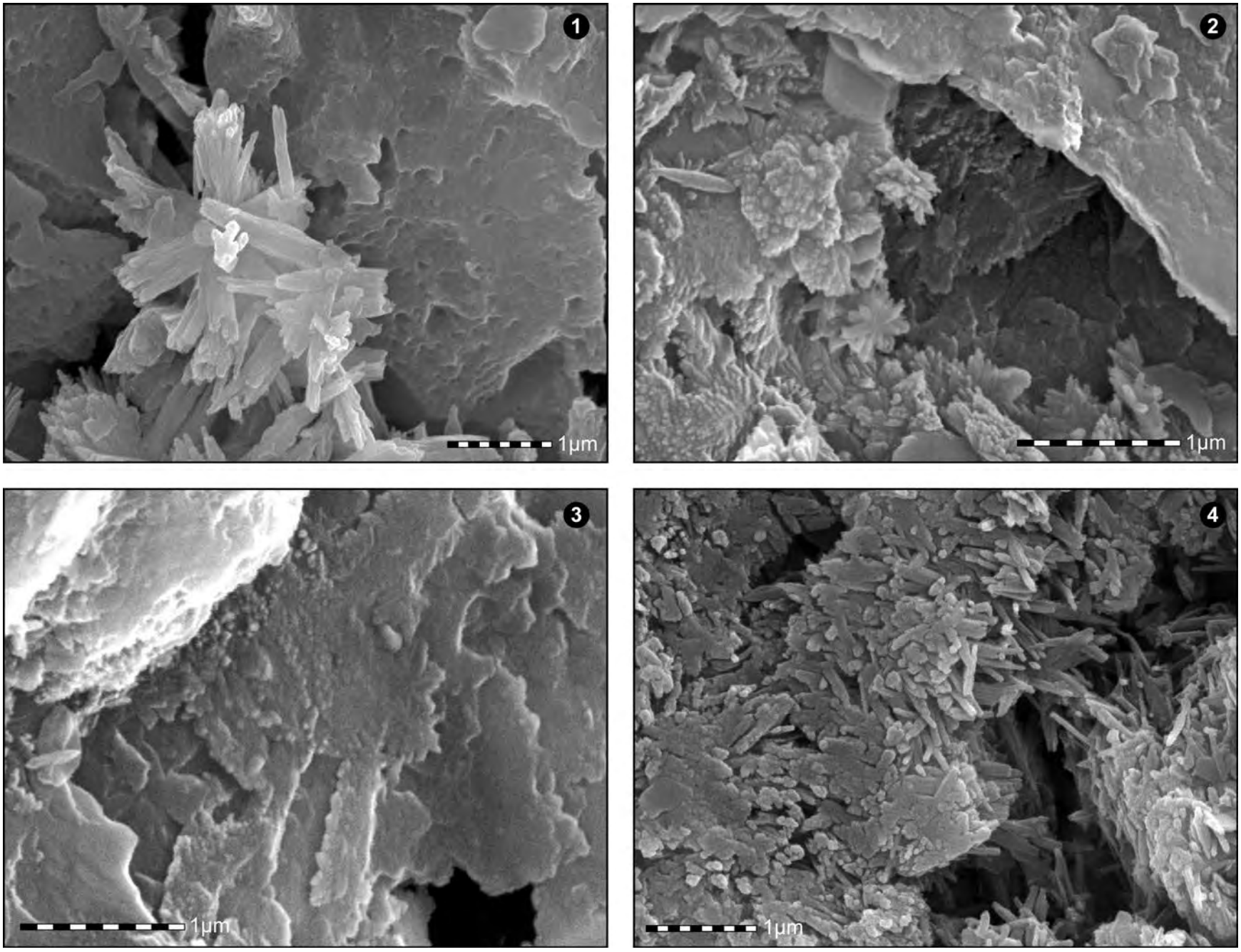
1
1µm
2
1µm
3
1µm
4
1µm

Plate 3

Fig. 1: Thin layers of goethite-rods and beads.
The rods and beads are loosely connected to each other. In the center, however, there is a more compact layer of spheres with a thickness of one bead.
Box: see Pl. 3, Fig. 2.

Fig. 2: Close-up of Fig. 1 (box).
In the middle and upper left, a layer of densely arranged minute spheres is present. At the right there are some rods and a lot of beads, which merge to slightly larger entities.
Gold cover: moderate thickness.

Fig. 3: Transition area from limestone to dolostone layer.
An ankerit crystal is covered by a thin layer of minute spheres at the right and by an accumulation of apatite crystals at the left.
Box: see Pl. 3, Fig. 4.

Fig. 4: Close-up of Fig. 3 (box).
The layer is made up almost entirely of loosely scattered minute spheres; rarely short rods are present as single individuals or forming star-like structures (arrows). This image suggests that the rods originate from the spheres. The structures are accentuated by the gold cover.
Gold cover: excess gold.

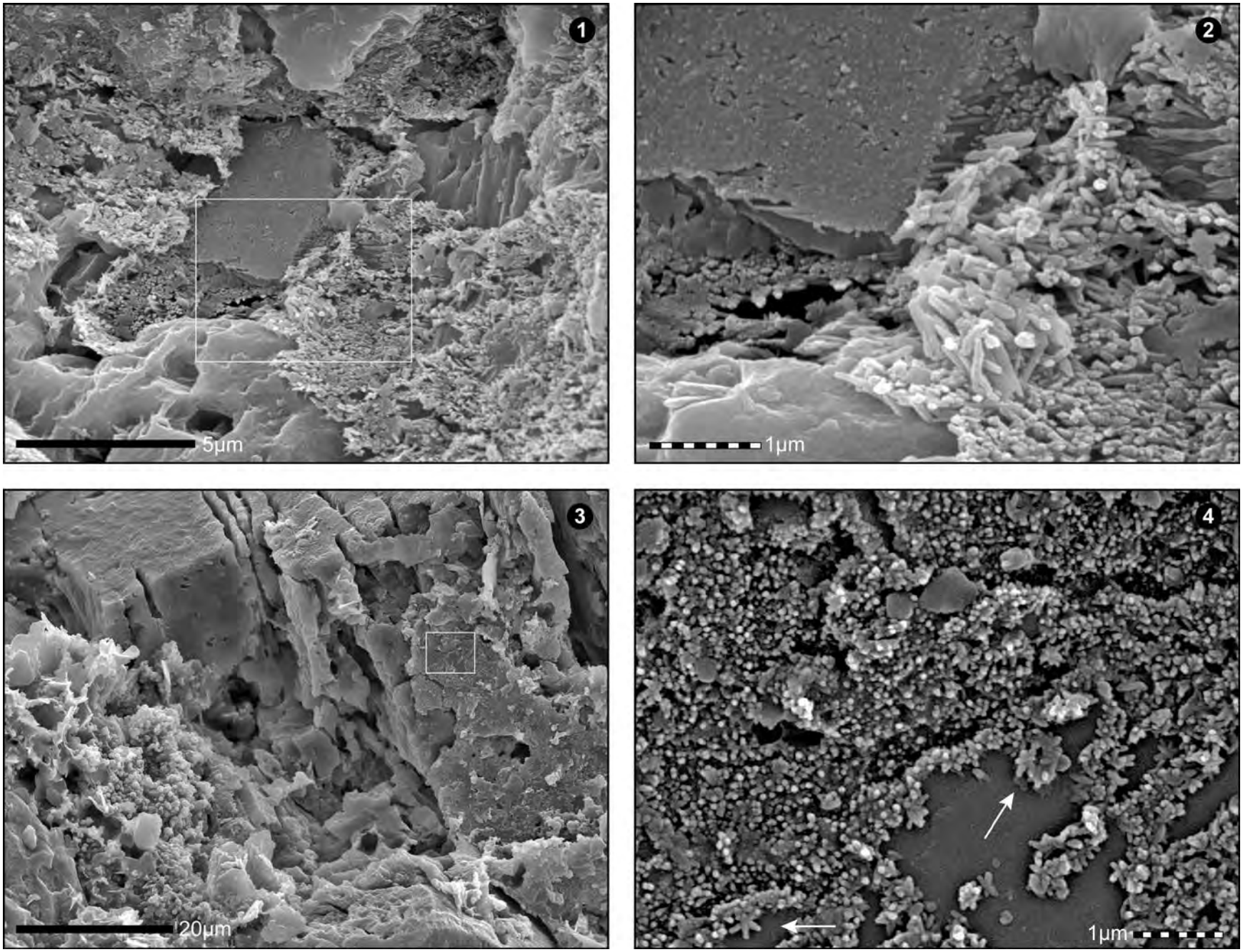
1
5µm
2
1µm
3
20µm
4
1µm

Plate 4

Fig. 1: Accumulation of goethite-rods and tiny beads.
The rods are of different lengths and occasionally rather short, thus suggesting that they originate from the beads. The structures are accentuated by the gold cover.
Gold cover: excess gold.

Fig. 2: Fe-oxide crystals, goethite-rods and tiny beads.
The crystals in the lower left are made up of beads. The goethite-rods in the upper right are present as single individuals or joined to bunches and are accompanied by minute spheres. The structures are accentuated by the gold cover.
Gold cover: excess gold.

Fig. 3: Fe-oxide framboid, covered by layers of illite.
A few goethite-rods and large quantities of tiny spheres occur in addition.
Gold cover: thin (30 seconds sputter-time).
Box: see Pl. 4, Fig. 4.

Fig. 4: Close-up of Fig. 3 (box).
Numerous minute beads are scattered across the framboid.
Gold cover: thin (30 seconds sputter-time).

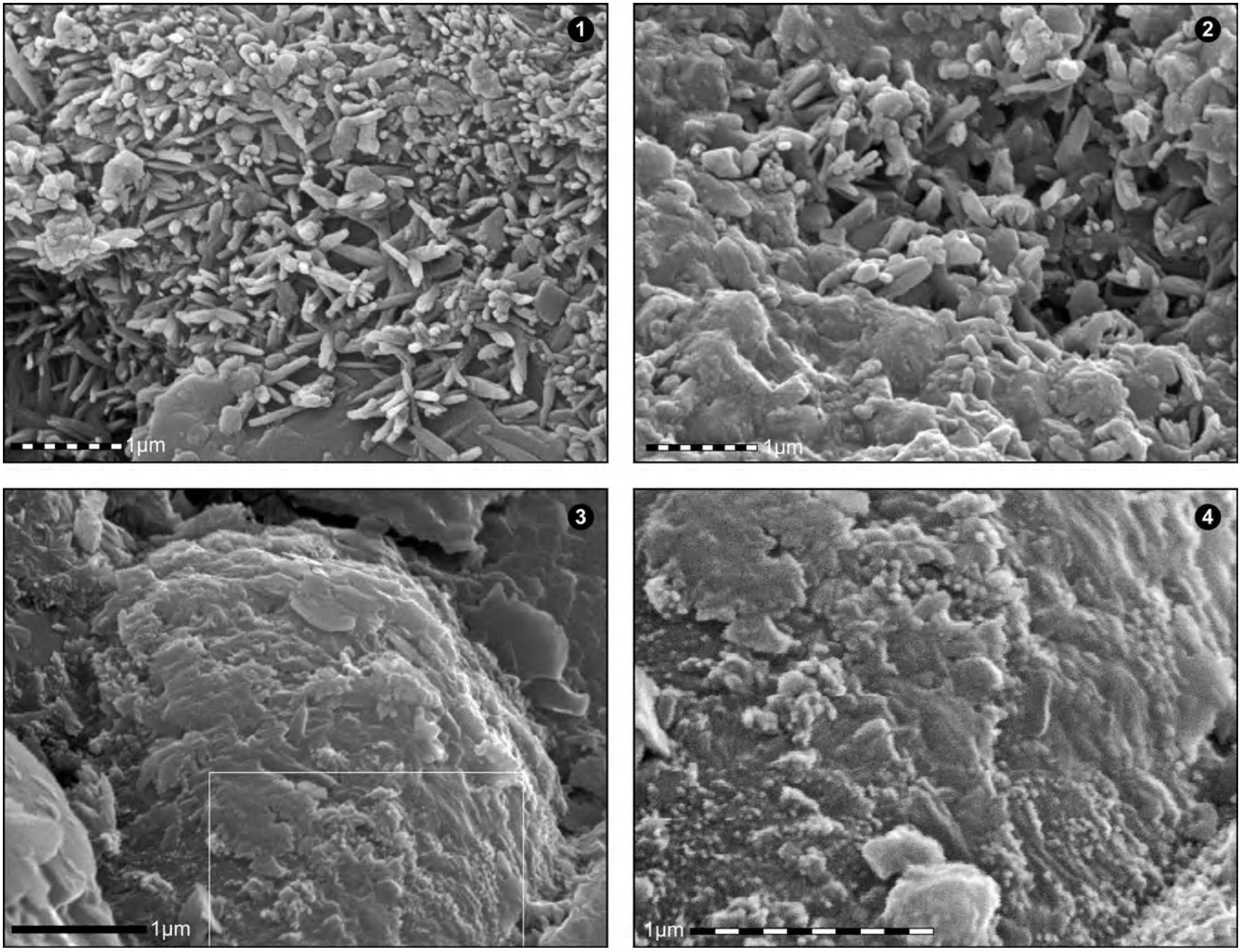
1
1µm
2
1µm
3
1µm
4
1µm

Plate 5

Fig. 1: Fe-oxide framboid with a coating of illite.
Also a few goethite-rods are present at the left side of the framboid. Left of the framboid, a thick layer of illite has been identified.
Box: see Pl. 5, Fig. 2.

Fig. 2: Close-up of Fig. 1 (box).
Both the clay minerals at the left and the Fe-oxide crystallites consist of closely arranged tiny spheres.
Gold cover: moderate thickness.

Fig. 3: Fe-oxide framboid.
The faces of some crystallites are smooth, but others show merging or loosely adjoining beads from which short goethite-rods are ariseing. In the centre and lower right the composition of the crystallites of thin layers is visible. EDX-analyses revealed that there are no chemical differences between the areas with rods and the smooth crystallites. The structures are accentuated by the gold cover.
Gold cover: excess gold.

Fig. 4: Fe-oxide framboid.
The faces of the crystallites are all covered with minute spheres. The structures are accentuated by the gold cover.
Gold cover: excess gold.

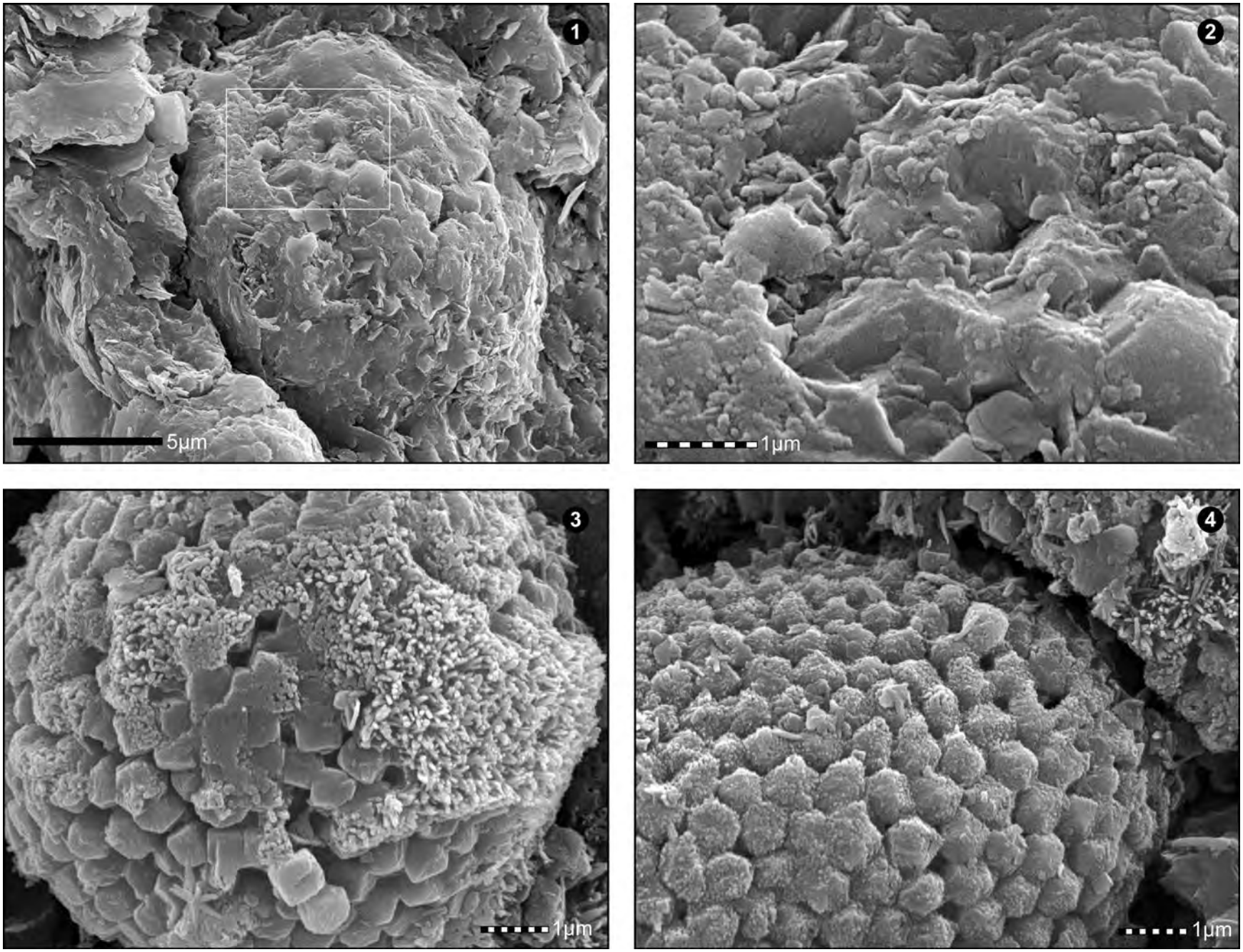
1
5µm
2
1µm
3
1µm
4
1µm

Plate 6

Fig. 1: Overview of a limestone sample.
The darker smooth areas are calcite. The light grey, spongy patches consist mainly of accumulations of fluorapatite crystals with embedded pyrite- and Fe-oxide-framboids, single crystals of pyrite, amorphous silica and various microfossils.

Fig. 2: Close-up of the surface of a calcite grain.
Minute spheres are arranged in dense rows and layers.
Gold cover: thin (30 seconds sputter-time).

Fig. 3: Fe-oxide framboid.
Most of the crystallites show smooth faces. In other areas, however, but mainly in the central part of the framboid, which seems to be yet uncompleted, it is clearly observable that the crystallites are built up by closely spaced beads.
Gold cover: thin (30 seconds sputter-time).

Fig. 4: Accumulation of various minerals.
Fe-oxide and pyrite framboids are accompanied by euhedral pyrite crystals of different sizes, thin layers of silica and fluorapatite crystals.
Box a: see Pl. 7, Fig. 1.
Box b: see Pl. 7, Fig. 3.
Box c: see Pl. 8, Fig. 1.

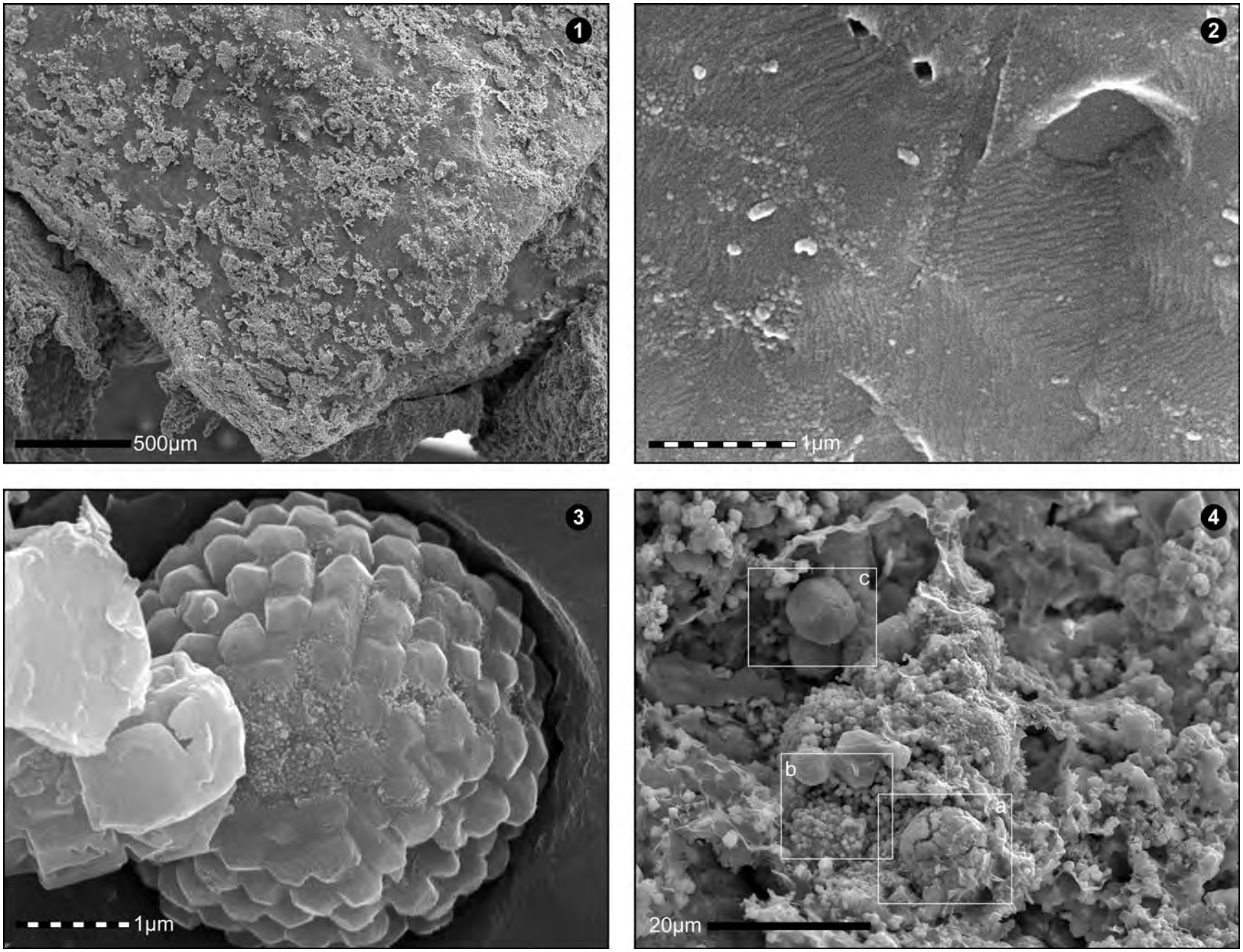
1
500µm
2
1µm
3
1µm
4
c
b
a
20µm

Plate 7

Fig. 1: Fe-oxide framboid.
Enlargement of Pl. 6, Fig. 4 (box a). The crystallites of the framboid are irregularly developed and partly covered by closely spaced tiny spheres and very short rods (upper left) and thin silica layers (lower right). Left to the framboid, euhedral pyrite crystals of various sizes are present.
Box: see Pl. 7, Fig. 2.

Fig. 2: Close-up of Fig. 1 (box).
Incrustation of the Fe-oxide framboid by densely packed beads and very short, thick rods. According to the EDX-analyses there are no differences in the chemical composition between the incrusted and the smooth areas.
Gold cover: thin (30 seconds sputter-time).

Fig. 3: Irregularely developed Fe-oxide framboid and euhedral pyrit crystals.
Enlargement of Pl. 6, Fig. 4 (box b). The framboid is surrounded by euhedral pyrite crystals of various sizes. In the upper left there is another Fe-oxide framboid, to its right a large euhedral Fe-oxide crystal.
Box a: see Pl. 7, Fig. 4.
Box b: see Pl. 8, Fig. 3.

Fig. 4: Close-up of Fig. 3 (box a).
At the left, tiny beads make up the crystallites, at the right also bunches of goethite-rods occur, some showing a radial arrangement, their axes form angles of 60°.
Gold cover: thin (30 seconds sputter-time).

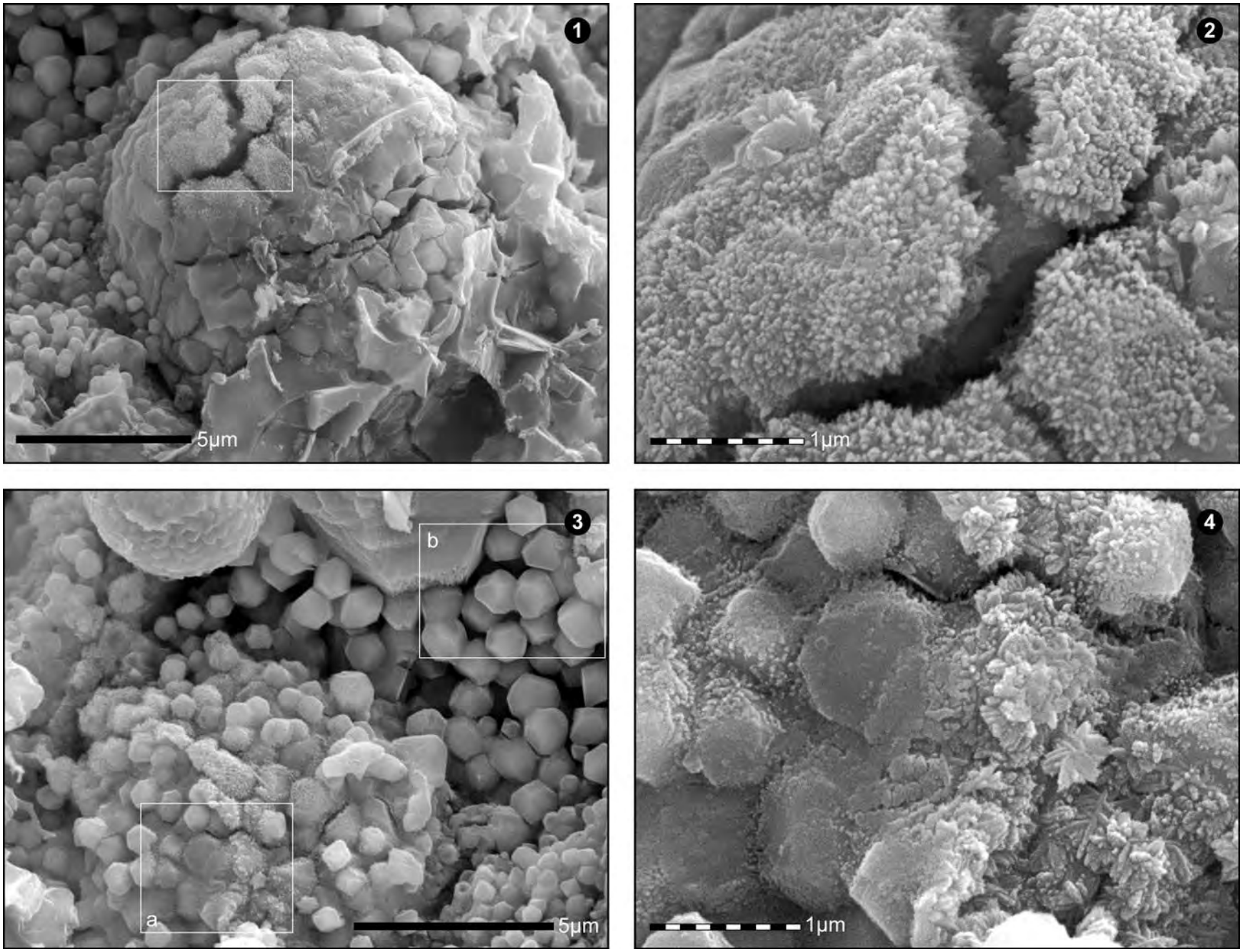
1
5µm
2
1µm
3
b
a
5µm
4
1µm

Plate 8

Fig. 1: Fe-oxide framboid.
Enlargement of Pl. 6, Fig. 4 (box c).
Box: see Pl. 8, Fig. 2.

Fig. 2: Close-up of Fig. 1 (box).
Some of the crystallites are developed as large, thin slabs which exhibit a granular structure. Also several of the normal crystallites reveal their composition of beads.
Gold cover: thin (30 seconds sputter-time).

Fig. 3: Euhedral pyrite crystals.
Close-up of Pl. 7, Fig. 3 (box b). Most of the crystals have smooth faces, but some seem to be unfinished and show a construction of closely packed spherules. In the upper left, a large Fe-oxide crystal is built up of thin layers of short rods and tiny beads.
Gold cover: thin (30 seconds sputter-time).

Fig. 4: Muellerisphaerida shell.
This microfossil of uncertain systematic position is embedded in calcite. At the left and in the central cavity of the fossil there are accumulations of mainly fluorapatite crystals accompanied by pyrite and Fe-oxide framboids, euhedral pyrite crystals and amorphous silica (s).
Box a: see Pl. 9, Fig. 1.
Box b: see Pl. 9, Fig. 2.

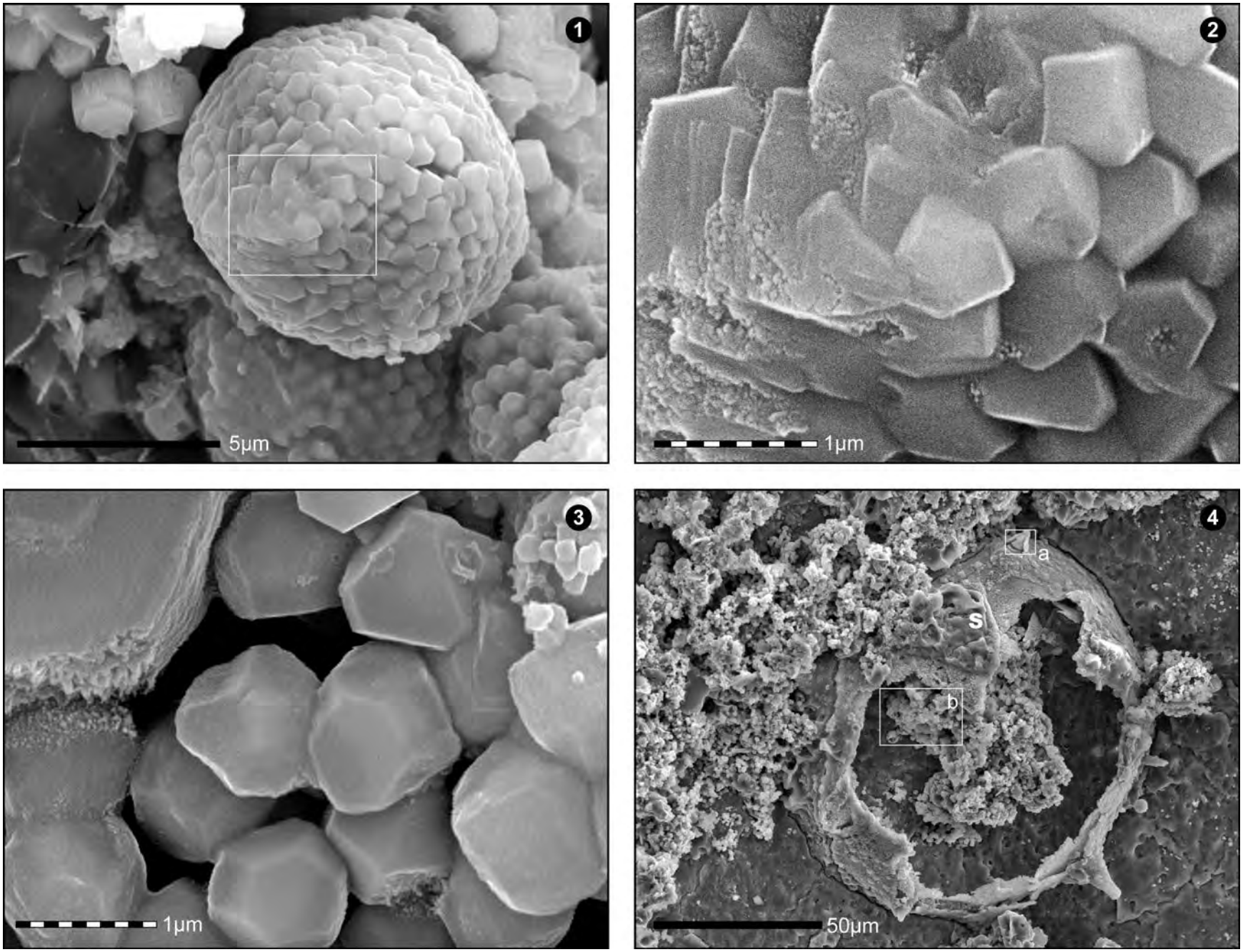
1
5µm
2
1µm
3
1µm
4
a
S
b
50µm

Plate 9

Fig. 1: Process of the Muellerisphaerida shell.
Close-up of Pl. 8, Fig. 4 (box a). The anhedral apatite crystals of the recrystallised shell show loosely scattered minute spheres.
Gold cover: thin (30 seconds sputter-time).

Fig. 2: Accumulation of fluorapatite crystals.
Enlargement of Pl. 8, Fig. 4 (box b). In the lower left there is an unfinished pyrite framboid, in the upper right a lump of silica (s).
Box: see Pl. 9, Fig. 3.

Fig. 3: Close-up of Fig. 2 (box).
The faces of euhedral fluorapatite crystals reveal closely spaced spherules.
Gold cover: thin (30 seconds sputter-time).

Fig. 4: Fluorapatite crystals.
Their growth apparently had been cut short. Minute spheres are strung together like a rosary (arrow). In the upper right spherules of the calcite are densely packed in rows and layers.
Gold cover: thin (30 seconds sputter-time).

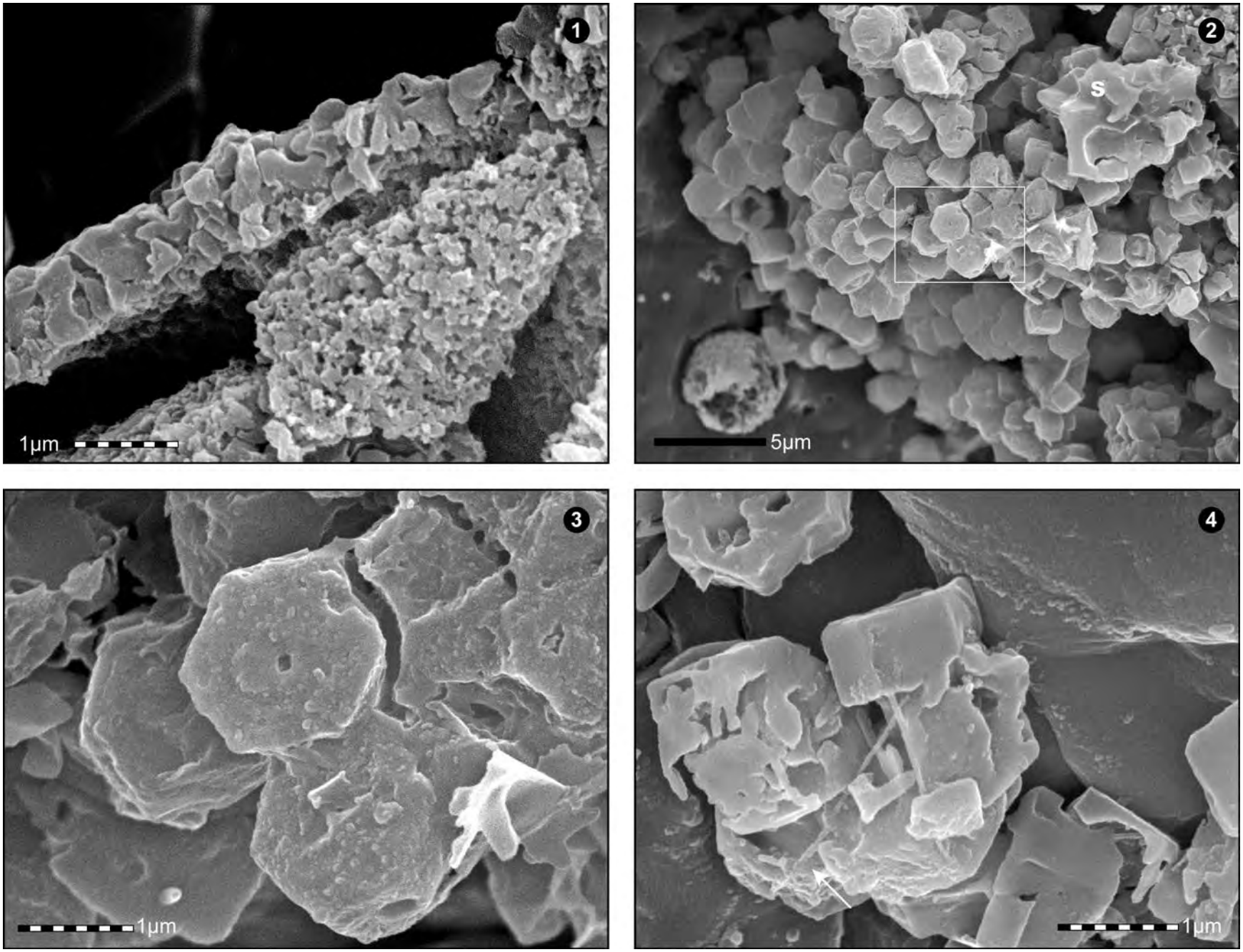
1
1µm
2
S
5µm
3
1µm
4
1µm

Plate 10

Fig. 1: *Eisenackitina krizi* PARIS & LAUFELD, 1980.
A chitinozoa that is embedded in calcite and surrounded by an accumulation of apatite crystals and amorphous silica.
Box: see Pl. 10, Fig. 2.

Fig. 2: Close-up of Fig. 1 (box).
The surface of the chitinozoa is covered by a thin inorganic coating which reveals loosely and patchy scattered tiny spheres.
Gold cover: thin (30 seconds sputter-time).

Fig. 3: *Eisenackitina krizi* PARIS & LAUFELD, 1980.
This chitinozoa has been obtained by palynological preparation of the rock sample. An – at the low magnification of a light microscope – web-like matter (inside and outside the box) is clinging to it.
Box: see Pl. 10, Fig. 4.

Fig. 4: Close-up of Fig. 3 (box).
The web-like appendage consists of minute spheres. EDX-analyses proved a chemical relationship to the coating of the chitinoza in situ (Pl. 10, Fig. 2).
Gold cover: moderate thickness.

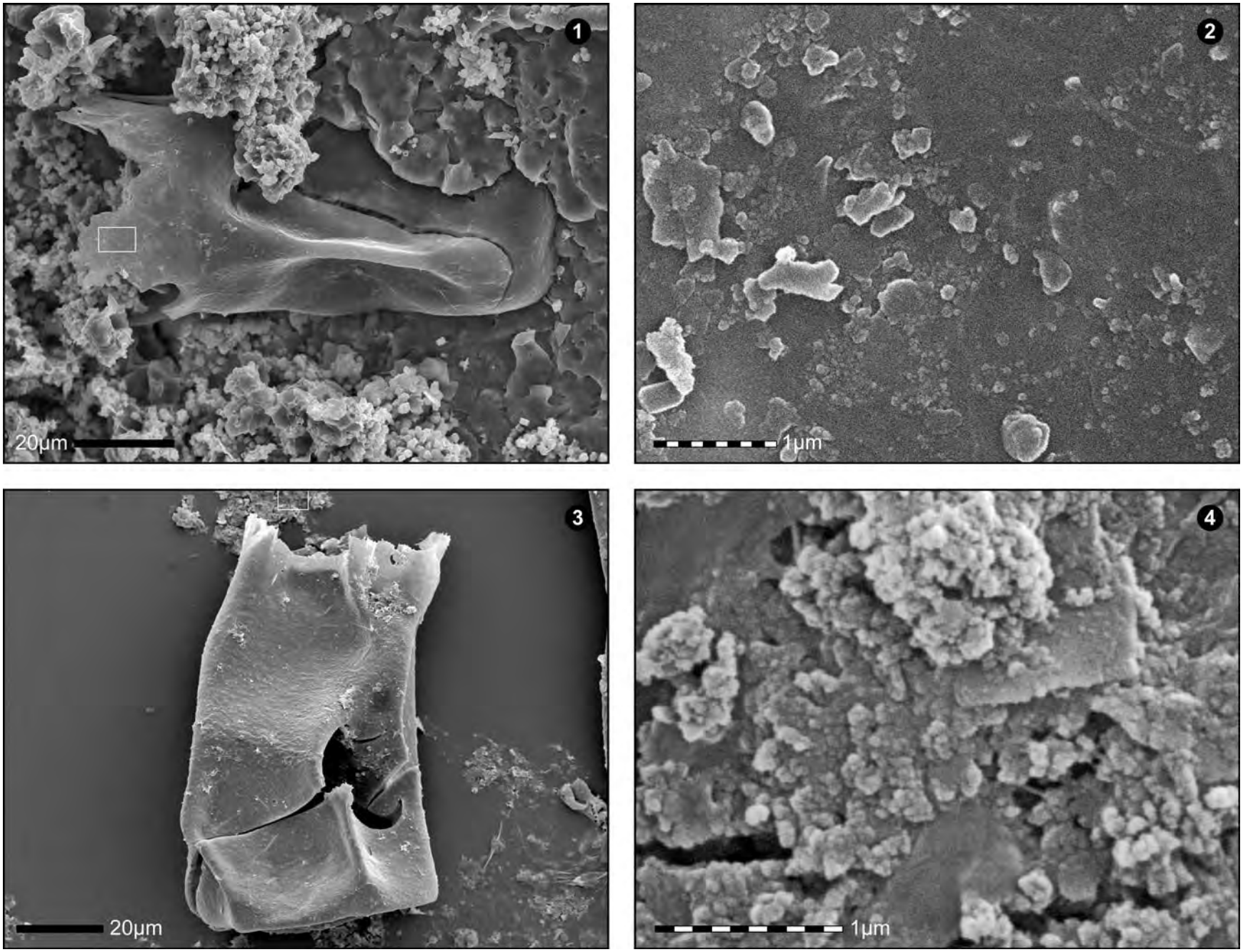
1
20µm
2
1µm
3
20µm
4
1µm

Plate 11

Fig. 1: Sheets of minute spheres.
They are situated close to large accumulations of apatite crystals on the surface of a limestone sample and are very similar to the accumulation of spherules in Pl. 10, Fig. 4. The bright minerals are apatite grains. The structures are accentuated by the gold cover.
Gold cover: excess gold.

Fig. 2: Surface of a piece of rock after palynological preparation.
The piece of rock has not been completely dissolved during palynological preparation. Minute calcium fluoride beads are present, which frequently coalesce to larger spheres and even form rosary like chains (arrow). The structures are accentuated by the gold cover.
Gold cover: excess gold.

Fig. 3: Microbe-like structures.
Peculiar structures are formed by minute calcium fluoride beads from a smashed piece of rock, which has not been completely dissolved during palynological preparation. The tiny beads merge to larger spheres; at first with granulate, then with smooth surfaces. Finally the smooth spheres join to pairs, thus imitating cell division. The structures are accentuated by the gold cover.
Gold cover: excess gold.

Fig. 4: Microbe-like structures.
When the coalescence of the calcium fluoride beads in Fig. 3 goes on, the larger spheres fuse to flat colonies of several to many discs with smooth surfaces. The structures are accentuated by the gold cover.
Gold cover: excess gold.

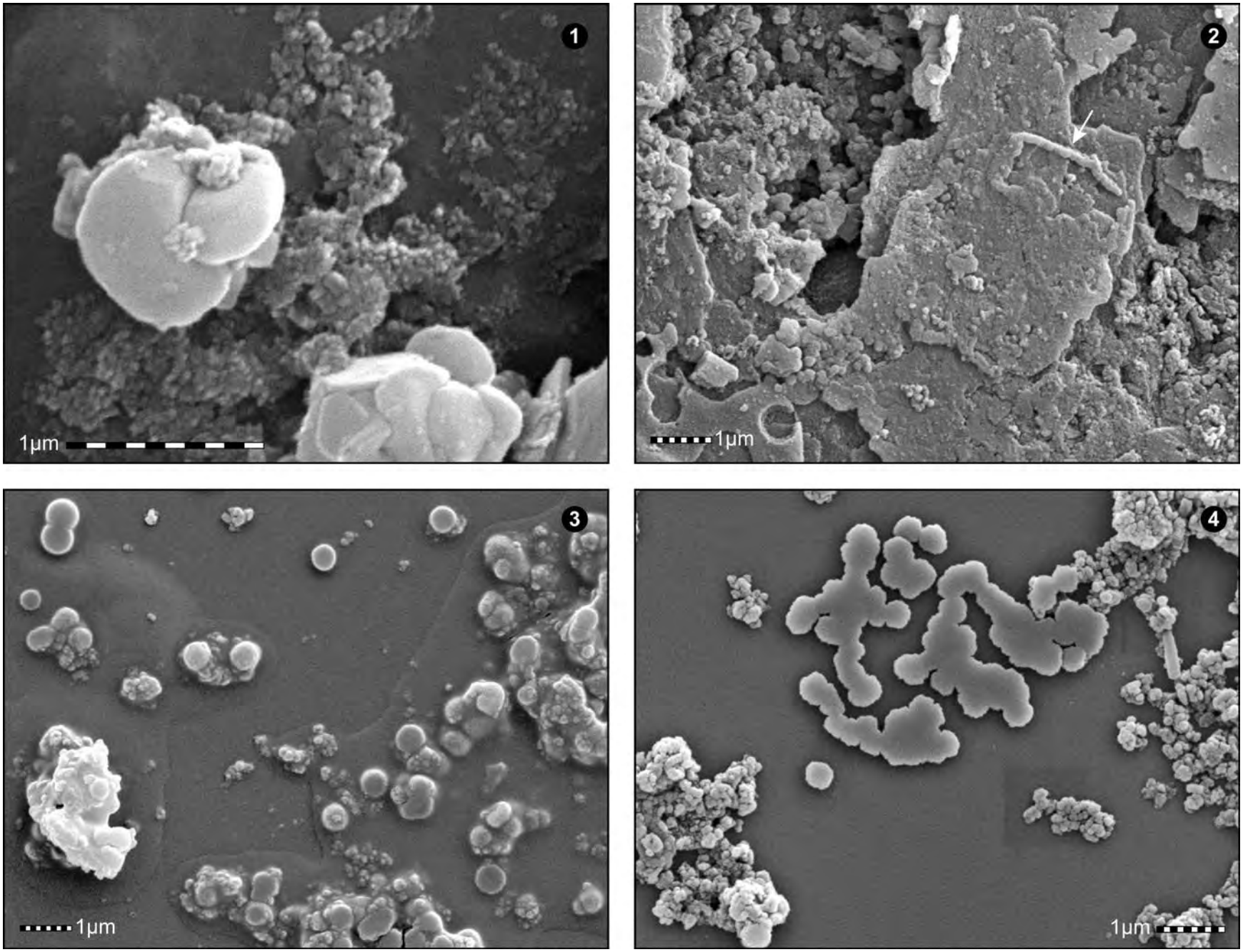
1
1µm
2
1µm
3
1µm
4
1µm

Plate 12

Fig. 1: Accumulation of tiny calcium fluoride spheres.
A smashed piece of rock, which has not been completely dissolved during palynological preparation, consists almost entirely of tiny calcium fluoride spheres. The spheres frequently merge to larger spherical units. The structures are accentuated by the gold cover.
Gold cover: excess of gold.

Fig. 2: Crystals of calcium fluoride.
After 4 hours in 51–54% hydrofluoric acid, pieces of the laminated calcisiltite sample were completely covered by small unfinished euhedral crystals of calcium fluoride.
Box: see Pl. 12, Figs. 3, 4.

Fig. 3: Close-up of Fig. 2 (box).
The incomplete calcium fluoride crystals are entirely composed of tiny spheres. They coalesce to thin layers and the layers one by one build up the crystals.
Gold cover: moderate thickness.

Fig. 4: Close-up of Fig. 2 (box).
Same as in Fig. 3, but with a double thickness of gold. Compared to Fig. 3, the sizes of the beads increased, but no new ones were formed. Only already existing structures were accentuated.
Gold cover: excess gold.

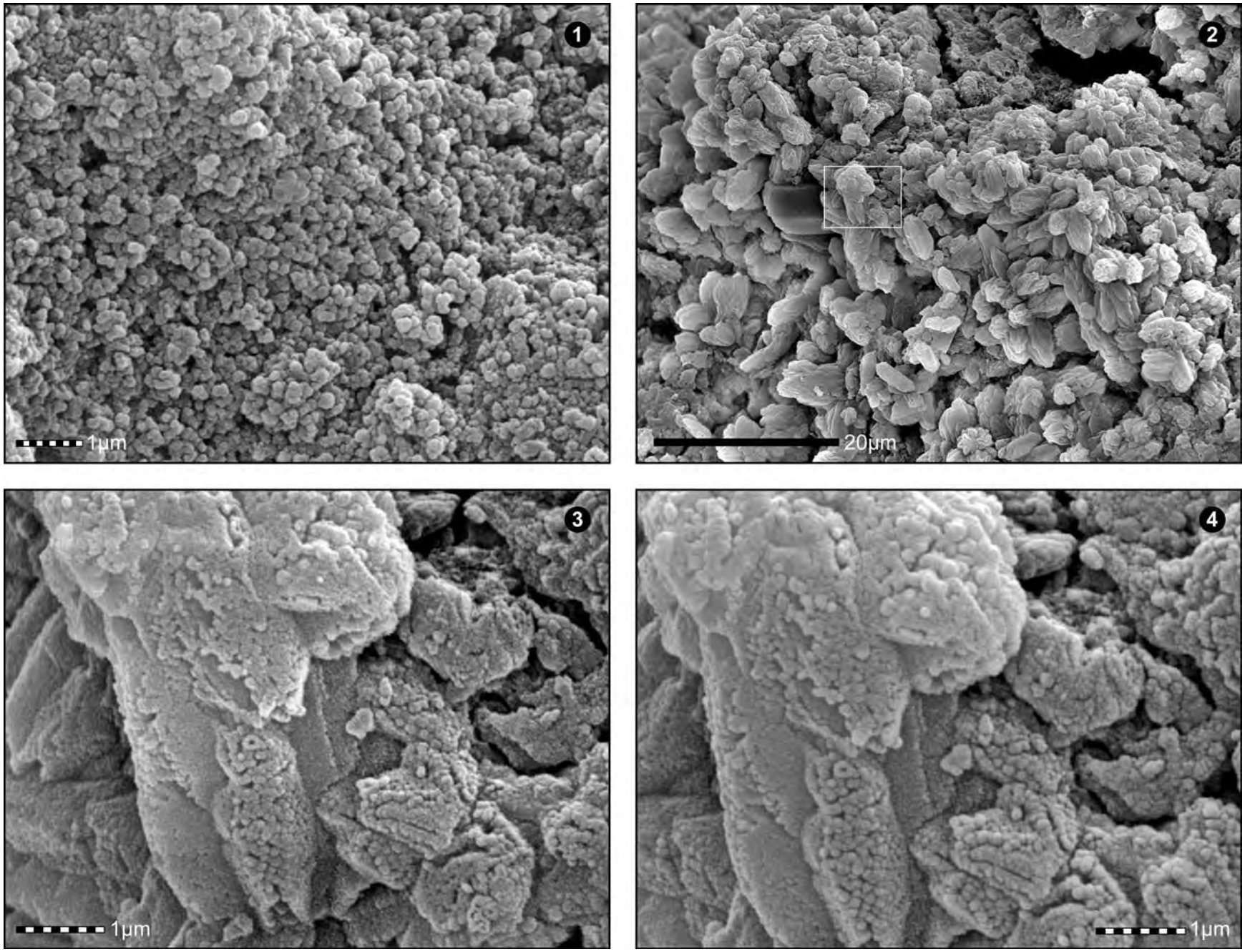
1
1µm
2
20µm
3
1µm
4
1µm